

## CLUES TO NUCLEAR STAR CLUSTER FORMATION FROM EDGE-ON SPIRALS

ANIL C. SETH\*

University of Washington, Astronomy Dept., Box 351580, Seattle, WA 98195

JULIANNE J. DALCANTON†

University of Washington, Astronomy Dept., Box 351580, Seattle, WA 98195

PAUL W. HODGE

University of Washington, Astronomy Dept., Box 351580, Seattle, WA 98195

VICTOR P. DEBATTISTA‡

University of Washington, Astronomy Dept., Box 351580, Seattle, WA 98195

*Accepted for publication in the Astronomical Journal*

### ABSTRACT

We find 9 nuclear cluster candidates in a sample of 14 edge-on, late-type galaxies observed with HST/ACS. These clusters have magnitudes ( $M_I \sim -11$ ) and sizes ( $r_{eff} \sim 3$  pc) similar to those found in previous studies of face-on, late-type spirals and dE galaxies. However, three of the nuclear clusters are significantly flattened and show evidence for multiple, coincident structural components. The elongations of these three clusters are aligned to within  $\sim 10^\circ$  of the galaxies' major axes. Structurally, the flattened clusters are well fit by a combination of a spheroid and a disk or ring, with the disk preferred in two of three cases. The nuclear cluster disks/rings have F606W-F814W ( $\sim V-I$ ) colors 0.3-0.6 magnitudes bluer than the spheroidal components, suggesting that the stars in these components have ages  $< 1$  Gyr. In NGC 4244, the nearest of the nuclear clusters, we further constrain the stellar populations via spectroscopy and multi-band photometry. This nuclear cluster is equally well fit by single-stellar populations with ages of either  $\sim 100$  Myr or  $\sim 1$  Gyr, and with masses of  $2-5 \times 10^6 M_\odot$ . However, significantly better fits to the spectroscopy and photometry are obtained by combining two or more stellar populations. Exploiting emission lines that appear to originate  $\sim 1''$  from the NGC 4244 nucleus, we determine a lower limit on the dynamical mass of  $2.5_{-1.2}^{+1.7} \times 10^6 M_\odot$  within 19 pc, typical of values found for other nuclear clusters. We also present tentative evidence that another of the nuclear clusters (in NGC 4206) may also host a supermassive black hole. Based on our observational results we propose an *in situ* formation mechanism for nuclear clusters in which stars form episodically in compact nuclear disks, and then lose angular momentum or heat vertically to form an older spheroidal structure. We estimate the period between star formation episodes to be  $\sim 0.5$  Gyr and discuss possible mechanisms for transforming the disk-like components into spheroids. We also note the connection between our objects and massive globular clusters (e.g.  $\omega$  Cen), ultra-compact dwarfs, and supermassive black holes.

*Subject headings:* galaxies:nuclei – galaxies:star clusters – galaxies:spiral – galaxies:formation – galaxies:individual (IC 5052, NGC 4244, NGC 4206)

### 1. INTRODUCTION

Due to their deep gravitational potential wells and unique dynamics, the centers of galaxies frequently host exotic objects such as supermassive black holes, active galactic nuclei, and massive stellar clusters. Of these, only nuclear star clusters provide a visible record of the accretion of stars and gas into the nucleus. Therefore, studies of nuclear star clusters hold the promise to shed light on the formation of central massive objects of all types.

Bright nuclear star clusters have been observed in  $\sim 75\%$  of the 77 face-on galaxies of type Scd and later

studied by Böker et al. (2002). Similar clusters appear to be frequent in earlier type spirals as well, although their study is complicated by the presence of bulges and other nuclear phenomena (Carollo et al. 2002). Dwarf elliptical galaxies, which may originate from low-mass spiral galaxies (e.g. Mastroiello et al. 2005; Beasley et al. 2006), also frequently possess nuclear star clusters (Grant et al. 2005; Côté et al. 2006).

In late-type spiral galaxies with little or no bulge, nuclear star clusters are very prominent and can be studied in detail. From their sample of face-on, late-type spiral galaxies, Böker et al. (2004) found that nuclear clusters have dimensions similar to Milky Way globular clusters, with typical half-light radii of 3.5 pc. However, these clusters are significantly brighter than globular clusters, with  $I$  band magnitudes ranging between  $-8$  and  $-16$  (Böker et al. 2002). Their high luminosities are

\*Currently a CfA Postdoctoral Fellow, 60 Garden St., Cambridge, MA 02138, aseth@cfa.harvard.edu

†Alfred P. Sloan Research Fellow

‡Brooks Prize Fellow

at least in part due to their large masses; Walcher et al. (2005) have used high-resolution spectra to derive typical masses  $\sim 3 \times 10^6 M_\odot$  for nine galaxies in the Böker et al. (2002) sample, similar in mass to the most massive Milky Way cluster,  $\omega$  Cen (Meylan & Mayor 1986). However, the brightness of nuclear clusters also results in part from the presence of young stellar populations. Photometry and spectra of a number of clusters suggest that nuclear clusters in both spiral and dwarf ellipticals have populations much younger than globular clusters (e.g. Ho et al. 1995; Lotz et al. 2004). In late-type galaxies, most clusters appear to have stars with ages  $< 100$  Myr (Walcher et al. 2006). Furthermore, recent spectral studies have shown that nuclear clusters are made up of composite stellar populations, with most having substantial old ( $\gtrsim 1$  Gyr) stellar component (Long et al. 2002; Sarzi et al. 2005; Walcher et al. 2006; Rossa et al. 2006).

Not only are nuclear clusters present in a large fraction of present day spirals and dwarf ellipticals, they also have been invoked as the progenitors of massive globular clusters and ultra-compact dwarfs. In a hierarchical merging scenario, many galaxies will be tidally stripped during mergers leaving behind only their dense nuclei (e.g. Bekki & Chiba 2004). Nuclear cluster properties match the half-light radii and exceptional luminosity of massive globulars and UCDs (Mackey & van den Bergh 2005; Phillipps et al. 2001; Jones et al. 2006). Furthermore, the multiple stellar populations seen in  $\omega$  Cen and G1 (e.g. Bedin et al. 2004; Meylan et al. 2001), and the evidence for possible self-enrichment among the brightest globular clusters in ellipticals (Harris et al. 2006) strengthen the association between these bright compact objects.

Finally nuclear clusters appear to be intimately connected to the formation of supermassive black holes (SMBHs) at the centers of galaxies. For both spiral and elliptical galaxies, a clear correlation is seen between nuclear cluster mass and bulge mass (Côté et al. 2006; Wehner & Harris 2006; Ferrarese et al. 2006; Rossa et al. 2006). This correlation appears to fall along the well-known  $M_\bullet - \sigma$  relation between black hole mass and bulge or galaxy mass (e.g. Ferrarese & Merritt 2000; Ferrarese 2002). Both SMBHs and nuclear clusters appear to contain the same fraction of the total galaxy mass, supporting the idea that they are two related types of central massive object (Wehner & Harris 2006). Whether a central massive object is a nuclear cluster or a SMBH appears to depend on mass; early-type galaxies more massive than  $\sim 10^{10} M_\odot$  appear to have SMBHs, while lower mass systems commonly host nuclear clusters (Ferrarese et al. 2006). These findings strongly suggest a similar formation mechanism for nuclear clusters and SMBHs. Increasing evidence also points to massive star clusters as sites of intermediate-mass black hole (IMBH) formation (e.g. Miller & Colbert 2004; Gebhardt et al. 2005; Patruno et al. 2006). These IMBHs may also follow the  $M_\bullet - \sigma$  relation (Gebhardt et al. 2002).

In this context, a detailed understanding of how nuclear clusters formed may reveal the general mechanism driving the formation of central massive objects of all types. Two basic scenarios have been suggested (e.g. Böker et al. 2004): (1) nuclear clusters form from multiple globular clusters accreted via dynamical friction (e.g. Tremaine et al. 1975; Lotz et al. 2001), and (2) nuclear

clusters form *in situ* from gas channeled into the center of galaxies (Milosavljević 2004). In this paper we present observational evidence that favors the *in situ* formation scenario. In particular, we find nuclear clusters that are elongated along the major axis of the galaxies and have two coincident components. These clusters appear to consist of a younger flattened disk or ring and an older spheroid. Based on the evidence we present, we suggest a detailed formation mechanism in which nuclear clusters form in repeated star formation events from very compact nuclear gas disks.

In §2 we describe the imaging and spectroscopic observations used in the paper. §3 focuses on an analysis of the morphology and luminosities of the clusters as revealed by HST observations. The stellar populations of the multiple-component clusters are examined in §4. In §5 we derive a dynamical mass for the NGC 4244 nuclear cluster, and then in §6 present tentative evidence that the NGC 4206 nucleus may harbor both a star cluster and a supermassive black hole. We present a detailed formation mechanism and discuss it in the broader context in §7, and then summarize our findings in §8.

## 2. OBSERVATIONS

### 2.1. Identification of Nuclear Clusters

Most of the data presented in this paper were taken with the Hubble Space Telescope’s (HST) Advanced Camera for Surveys (ACS) as part of a Cycle 13 snapshot program. Sixteen galaxies were observed in both the F606W and F814W filters, with exposure times of  $\sim 700$  seconds. Details of these observations and their reduction are presented in Seth et al. (2005) (Paper I).

We identified nuclear clusters (NCs) by careful examination of the central regions of our galaxies. The exact locations of the galaxy centers were determined using fits to 2MASS data presented in Paper I. Nuclear clusters were distinguished based on their proximity to the photocenter of the galaxy, their brightness/prominence, and their extent (i.e. if they appeared resolved). At the distance of most of our galaxies, NCs such as those observed by Böker et al. (2002) should be at least partially resolved.

Table 1 lists the galaxies in our sample and whether each possesses a NC (shown in the fifth column). In two of the sixteen galaxies in the sample, the central region was not covered by the ACS images (denoted with a “N/A” in Table 1). Of the remaining 14 galaxies, seven have prominent and/or extended sources located within  $\sim 2$  arcseconds of the photometric center of the galaxy. Another two have possible detections of NCs, where the candidate clusters were not very prominent (denoted with a “Maybe”). The remaining five galaxies have no obvious candidate NCs. Of these five definite non-detections, three (IRAS 06070-6147, IRAS 07568-4942, & NGC 4631) are in galaxies where strong dust lanes could have easily obscured any extant cluster. The other two of the non-detections (NGC 55 and IC 2233) are in low mass galaxies without strong dust lanes, suggesting that these galaxies truly lack NCs.

In summary, we have detected candidate NCs in 50% to 65% of our sample. Eliminating the galaxies with strong dust lanes, the fraction of galaxies with detected NCs may be as high as 82%. These detection fractions are consistent with other studies, both for late-type galax-

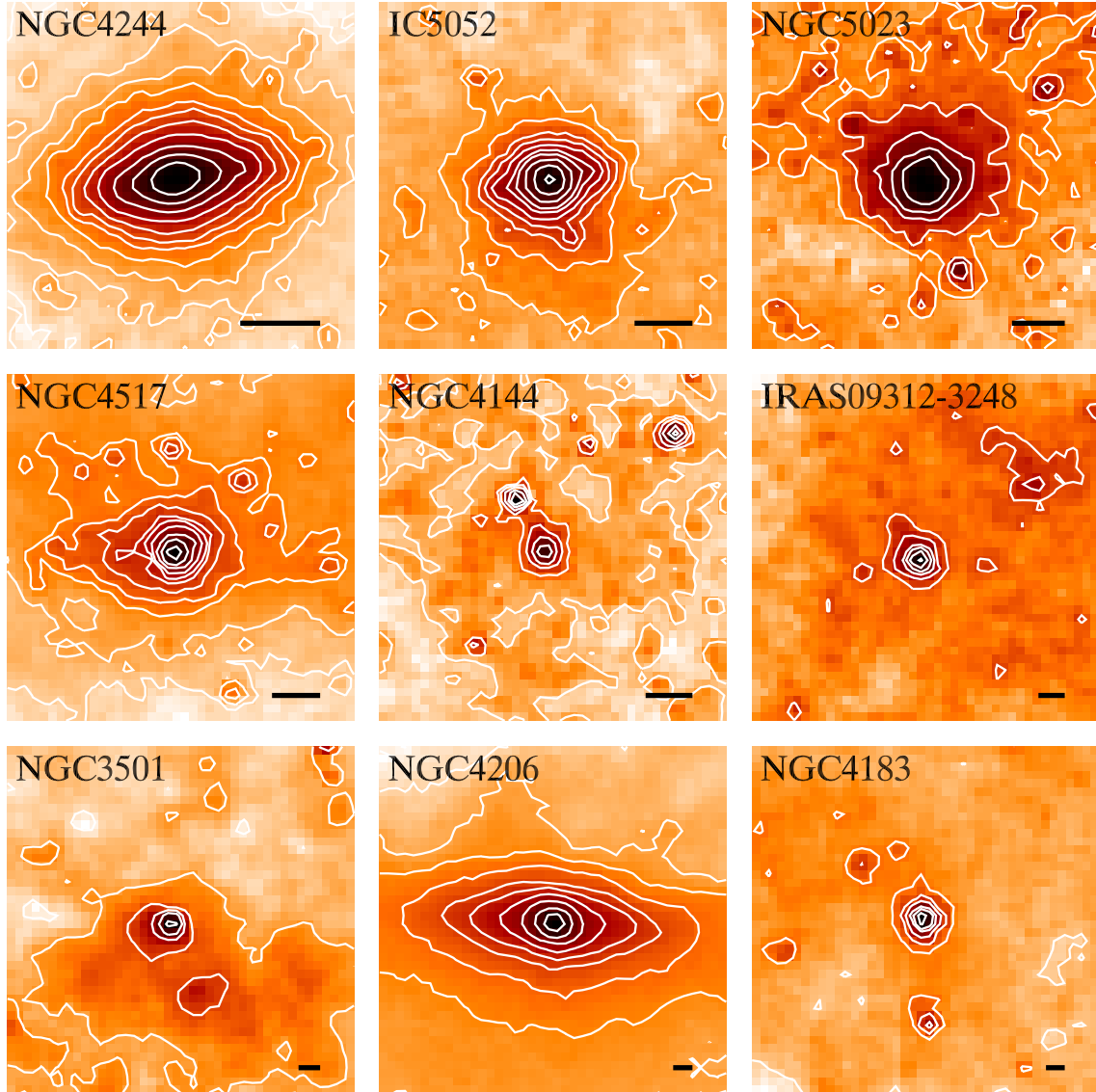


FIG. 1.— Images in the F814W filter of the nine candidate nuclear clusters. Each image is  $2''$  on a side, and the bar in the bottom right corner indicates a length of 10 pc. Images have been rotated so that the x-axis lies along the position angle of the major axis of the galaxy disk.

ies, where Böker et al. (2002) finds  $\sim 75\%$  of systems have clusters, and for early-type galaxies observed as part of the ACS Virgo Cluster Survey (Côté et al. 2006). However, our sample is less well-suited than these studies for constraining the frequency of nuclear clusters because the edge-on perspective can result in more chance superpositions and greater obscuration from dust.

## 2.2. Apache Point Observatory 3.5-m Spectrum

To better constrain the stellar populations of the NGC 4244 nuclear cluster (the nearest in our sample), we obtained long-slit spectra on May 19, 2005 with the Double Imaging Spectrograph (DIS) on the Apache Point Observatory (APO) 3.5m telescope. The DIS spectrograph obtains both blue and red spectra simultaneously. We used the “medium-resolution” blue grating ( $1.22\text{\AA}/\text{pixel}$ ) and the “high-resolution” red grating ( $0.84\text{\AA}/\text{pixel}$ ). The resulting images had good quality

spectral coverage from  $3700\text{\AA}$  to  $5500\text{\AA}$  on the blue side and  $5600\text{\AA}$  to  $7200\text{\AA}$  on the red side. A  $1.5''$  slit was used. Two exposures of 15 and 30 minutes were obtained centered on the nuclear cluster and oriented along the major axis of NGC 4244 with a position angle of  $-43^\circ$ . We note that the elongation of the nuclear cluster is aligned to within  $\sim 10^\circ$  of the galaxy’s major axis (see Fig. 1). Seeing at the time of observation was  $\sim 1.0''$ , and thus the cluster was essentially unresolved. We reduced these spectra using a PyRAF pipeline designed for DIS data reduction (written by Kevin Covey) which utilizes standard IRAF ONEDSPEC and TWODSPEC routines. The NGC 4244 cluster observations were wavelength calibrated using lamp spectra, and a further correction was applied to remove small shifts visible in the sky lines. The velocities were calibrated to the local standard of rest using RVCORRECT and DOPCOR. Observations of Feige 66 at nearly identical airmass were obtained for

TABLE 1  
GALAXY SAMPLE AND NUCLEAR CLUSTER PROPERTIES

Galaxy	Type	$M_B$	$V_{max}$ [km/sec]	Possess NC	Multiple Components	$M_{F814W}$	$m_{F606W} - m_{F814W}$	m-M
IC 2233	SBcd	-16.60	79	No	N/A			29.96 <sup>b</sup>
IC 5052	SBcd	-17.23	79	Yes	Yes	-10.77	1.08	28.90 <sup>a</sup>
IRAS 06070-6147	Sc	-20.50	133	No;Dust	N/A			31.22 <sup>d</sup>
IRAS 07568-4942	Sbc	-17.70	142	No;Dust	N/A			30.06 <sup>c</sup>
IRAS 09312-3248	Sc	-17.90	98	Maybe	No	-9.24	1.36	30.61 <sup>d</sup>
NGC 55	SBm	-17.05	67	No	N/A			26.63 <sup>a</sup>
NGC 891	Sb	-18.78	214	N/A	N/A			29.61 <sup>e</sup>
NGC 3501	Sc	-17.37	136	Yes	No	-10.58	1.62	31.04 <sup>d</sup>
NGC 4144	Sbc	-17.20	67	Maybe	No	-8.33	0.85	29.36 <sup>a</sup>
NGC 4183	Sc	-18.41	103	Yes	No	-11.15	0.93	31.35 <sup>f</sup>
NGC 4206	Sbc	-18.46	124	Yes	Yes	-14.17	0.93	31.29 <sup>g</sup>
NGC 4244	Sc	-17.08	93	Yes	Yes	<-12.65 <sup>i</sup>	0.77	28.20 <sup>a</sup>
NGC 4517	Sc	-18.18	137	Yes	Maybe	-11.34	1.77	29.30 <sup>c</sup>
NGC 4565	Sb	-20.47	227	N/A	N/A			31.05 <sup>h</sup>
NGC 4631	SBcd	-19.75	131	No;Dust	N/A			29.42 <sup>a</sup>
NGC 5023	Sc	-16.29	77	Yes	Maybe	-9.79	1.26	29.10 <sup>a</sup>

NOTE. — Types and velocities from HYPERLEDA/LEDA (Paturel et al. 1995, 2003). (a) Seth et al. (2005) (b) Bottinelli et al. (1985), (c) Bottinelli et al. (1988), (d) assuming  $H_0=70$  km/sec, (e) Tonry et al. (2001), (f) Tully & Pierce (2000), (g) Gavazzi et al. (1999), (h) Jensen et al. (2003) (i) The derived magnitudes on the NGC 4244 cluster are lower limits due to the central pixels being saturated in both bands.

flux calibration shortly before the observations; however the night was not photometric and thus the absolute flux scale is not fully constrained. The two observations of the NGC 4244 cluster differ in flux scale by under 10%, and our absolute flux is probably uncertain by a similar amount. Combined, the two spectra give a S/N of  $\sim 35$  per pixel. The cluster spectrum was extracted from within a  $2''$  diameter aperture, and regions used to define the background subtraction were within the confines of the galaxy,  $20''$ - $30''$  ( $\sim 1/4$ th the scale length of the galaxy) along the major axis in both directions. Any contamination from the underlying galaxy component should be very small, as the source was well above the background at all wavelengths. We analyze this data in §4 and §5.

### 3. NUCLEAR CLUSTER MORPHOLOGIES AND LUMINOSITIES

The most basic result of this paper is that nuclear clusters are not all simple, single-component objects, as is evident from inspection of Figure 1, which shows the F814W images of all nine nuclear cluster candidates. Of these candidates three (IC 5052, NGC 4206, & NGC 4244) look like miniature S0 galaxies, possessing both an elongated disk or ring component and a spheroidal component. These components are both compact with physical dimensions of tens of parsecs or less. We will show in §3.1.3 that these components appear to physically overlap. We therefore refer to these clusters as multi-component clusters throughout the rest of the paper. Two other galaxies, NGC 4517 & NGC 5023 also show tentative evidence for similar structures. In this section we focus on modeling the morphology of the clusters, in particular those that have multiple components. We will show: (1) the nuclear cluster elongations are closely aligned with the disk of the host galaxy, (2) models with both a spheroidal and disk or ring components fit the multi-component clusters significantly better than single-component models, and (3) the nuclear clusters in

our sample have magnitudes and sizes similar to those observed in other galaxies.

#### 3.1. Model fitting

The dimensions and scales of the clusters were determined via 2-D fitting to analytical functions (e.g. King profiles). Because the objects are very compact, it was necessary to include the effects of the PSF. We used two similar methods to fit the nuclear clusters. First, we used the *ishape* program (Larsen 1999), which was designed to fit semi-resolved clusters. Unfortunately, *ishape* only works with elliptically symmetric objects, which some of our objects clearly are not. Therefore, we wrote our own code in IDL, using the existing MPFIT2DFUN package to perform Levenberg-Marquardt least squares fits.

In both *ishape* and our program, analytical functions are convolved with the PSF before fitting to the data. We performed this convolution using a position-variable PSF derived from our data (see Paper I for details), and over-sampled by a factor of 10 to minimize the effects of aliasing and binning. A separate PSF was generated for each cluster based on its position on the chip. We conducted tests to insure that our program give similar results to the *ishape* program.

We used *ishape* (1) to determine what types of functions best fit the data, and (2) to assess if each cluster is indeed resolved. We fit Gaussian, King, Moffat, and Hubble profiles to each cluster and found that King and Moffat profiles provided the best overall fits in terms of the reduced  $\chi^2$ , as also found by Böker et al. (2004). Both profiles provided equally good fits to our clusters, and we chose to continue our fitting with elliptical King profiles of the form:

$$\Sigma(z) = \Sigma_0 \left( \frac{1}{\sqrt{1 + \left(\frac{z}{r_{core}}\right)^2}} - \frac{1}{\sqrt{1 + \left(\frac{r_{tidal}}{r_{core}}\right)^2}} \right) \quad (1)$$

$$\text{with } z = \sqrt{x^2 + \left(\frac{z}{q}\right)^2}$$

where  $\Sigma(z)$  is the projected surface brightness,  $x$  and  $z$  are the coordinates along the major and minor axes, and  $q$  is the axial ratio (minor/major). We have fixed the concentration ( $c \equiv r_{tidal}/r_{core}$ ) to be 15 for our fits, based on the fit concentrations of our brightest clusters and similar to that found for Galactic analog  $\omega$  Cen (Trager et al. 1995). We report only half-light/effective radii as this quantity is well determined even for relatively low signal-to-noise data (Carlson & Holtzman 2001), and does not depend strongly on the chosen model (see Fig. 2, Böker et al. 2004).

Given sufficient signal-to-noise, semi-extended sources can be detected with intrinsic widths as small as 10% of the PSF (Larsen 1999). The FWHM of our PSF is  $\sim 0.9$  pixels, meaning objects with widths smaller than a pixel should be easily resolvable. The signal-to-noise of our fits ranged from  $\sim 50$ -1500. For four of the galaxies (IC 5052, NGC 4206, NGC 4244, & NGC 5023), the FWHM of the fitted *ishape* King profiles is greater than one pixel, and the objects are clearly partially resolved. The  $\chi^2$  values of these fits is 2-20 times better than the  $\chi^2$  of a point-source fit (see last column, Table 2). The remaining fits have FWHM  $> 0.2$  pixels, and have  $\chi^2$  values 1-3 $\times$  the best-fitting point-source  $\chi^2$ . Of these, NGC 4144 and NGC 4517 are still clearly resolved, while IRAS 09312-3248, NGC 3501, & NGC 4183 (all of which are at large distances) are only marginally resolved.

### 3.1.1. Elliptical King Model Fits

Table 2 shows the results of our program's fits to single-component elliptical King profiles with  $c = 15$ . These fits show:

1. All the well resolved clusters are flattened, as shown in Figure 2. The median axis ratio ( $q \equiv b/a$ ) is 0.81, with  $q \sim 0.4$  for NGC 4206 and NGC 4244, the two systems with the most prominent disk (see §3.1.2).
2. The position angle of the three multi-component nuclear clusters (IC 5052, NGC 4206, & NGC 4244) are all aligned within 10 degrees of the galaxy disk position angle. This can be seen plainly in Figures 1 and 2. The NGC 4517 and NGC 5023 clusters also are somewhat elongated along the plane of the galaxy.
3. The effective radius (also known as the half-light radius) ranges between 1 and 20 pc, with most of the clusters having effective radii between 1-4 pc. Figure 3 demonstrates that the measured effective radii are similar to those observed for other objects including late-type nuclear clusters (filled circles Böker et al. 2004) and galactic globular clusters (open triangles Harris 1996).
4. After subtraction of the King profile fit, the residuals of IC 5052, NGC 4206, and NGC 4244 clearly show evidence for a flat disk- or ring-like component (see the middle column of Fig. 4). The reduced  $\chi^2$  of these three galaxies is also very high,

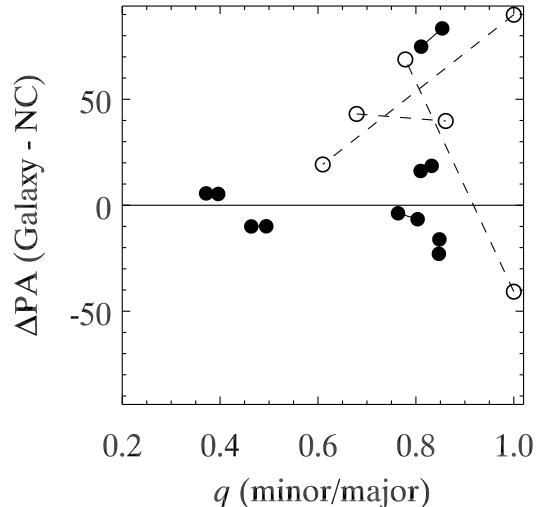


Fig. 2.— Elliptical King profile fit results: the axial ratio  $q$  is plotted against the position angle of the major axis of the nuclear cluster relative to the galaxy angle ( $\Delta\text{PA}$ ). The connected data points connect the fits for each galaxy in the two filters. Open circles indicate the three galaxies (IRAS09312-3248, NGC 3501, NGC 4183) for which good fits were not achieved, due to the NC compactness and complexity of the surrounding emission. This figure shows that most of the clusters we have detected were significantly flattened, and that the flattening aligns closely with the plane of the galaxy.

suggesting that the single component King profile is not a good fit to the data. We note that NGC 4517, which has a disk-like appearance in its outer isophotes, also has a high  $\chi^2$  value. In NGC 4244 the central eight pixels were saturated and therefore excluded from the fit.

### 3.1.2. Elliptical King + Disk Models

To account for the flattened residuals remaining after fits to the elliptical king profiles in the IC 5052, NGC 4206, and NGC 4244 nuclear clusters, we have fit an additional morphological component to these clusters. In this section we examine fits to disk models, in the next section we consider fits to ring models and compare the disk and ring fits.

As a disk model we adopted the surface brightness profile of a transparent, self-gravitating, edge-on exponential disk (van der Kruit & Searle 1981):

$$\Sigma(x, z) = \Sigma_0 \frac{x}{h_x} K_1 \left( \frac{x}{h_x} \right) \text{sech}^2 \left( \frac{z}{z_0} \right) \quad (2)$$

where  $x$  and  $z$  are the major and minor axis coordinates,  $\Sigma_0$  is the central surface brightness,  $K_1$  is the modified Bessel function,  $h_x$  is the disk's exponential scale length and  $z_0$  is the scale height of the disk. We note that we tried other vertical profile fits (e.g. simple exponential) which were too concentrated near the midplane to provide good fits to the data.

Figure 4 shows that the inclusion of a disk component clearly improves the fit relative to the single component elliptical King profile. Quantitatively, the  $\chi^2$  of the fits shown in Table 3 is significantly reduced relative

TABLE 2  
ELLIPTICAL KING PROFILE FITS

Galaxy	Pix. Scale [pc/pixel]	Filter	$r_{eff}$ [pc]	$q$ ( $b/a$ )	$\Delta PA^a$ [ $^\circ$ ]	Reduced $\chi^2$	$\chi_{PS}^2/\chi^2$ [ishape]
IC 5052	1.46	F606W	3.64	0.76	-3.8	23.8	5.78
IC 5052	1.46	F814W	2.93	0.80	-6.6	18.1	7.00
IRAS 09312-3248	3.21	F606W	2.46	0.68	43.1	2.8	1.50
IRAS 09312-3248	3.21	F814W	2.24	0.86	39.8	3.5	1.42
NGC 3501	3.91	F606W	6.82	1.00	89.9	8.2	1.41
NGC 3501	3.91	F814W	3.58	0.61	19.2	10.1	1.38
NGC 4144	1.81	F606W	1.46	0.85	83.4	3.2	2.69
NGC 4144	1.81	F814W	1.99	0.81	74.8	4.6	2.30
NGC 4183	4.51	F606W	2.76	1.00	-40.8	9.6	1.20
NGC 4183	4.51	F814W	3.02	0.78	68.8	6.4	1.12
NGC 4206	4.39	F606W	16.30	0.37	5.6	54.7	2.39
NGC 4206	4.39	F814W	15.81	0.40	5.3	42.4	2.75
NGC 4244	1.06	F606W	2.92	0.46	-10.0	94.1	20.73
NGC 4244	1.06	F814W	3.35	0.49	-9.9	82.3	19.63
NGC 4517	1.76	F606W	1.71	0.85	-22.9	46.0	1.20
NGC 4517	1.76	F814W	1.33	0.85	-16.1	64.2	1.23
NGC 5023	1.60	F606W	12.54	0.81	16.2	13.4	4.27
NGC 5023	1.60	F814W	10.22	0.83	18.6	11.1	6.89

NOTE. — (a)  $\Delta PA$  is the position angle relative to the galaxy disk.

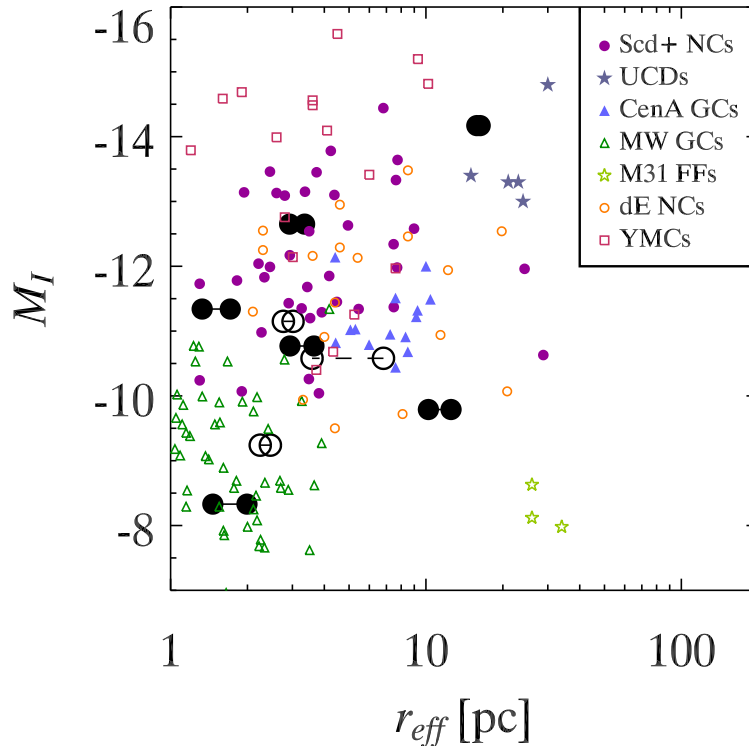


FIG. 3.— The fitted effective radius vs. the absolute aperture magnitude in the F814W filter. Large filled and open circles as in Fig. 2. Small symbols denote the following: *Filled circles* – late-type nuclear clusters from Böker et al. (2004). *Open circles* – dE,N nuclei from De Propriis et al. (2005) (transformed to  $M_I$  using Padova models which suggests stellar populations older than 1 Gyr have F814W-F850LP colors of  $0.25 \pm 0.1$  mags). *Filled triangles* – massive globular clusters in NGC 5128 observed by Martini & Ho (2004). *Open triangles* – Galactic globular clusters from the Harris (1996) catalog (note that  $\omega$  Cen is the brightest of these). *Filled Stars* – Fornax UCDs from Drinkwater et al. (2003), assuming V-I of  $1.1 \pm 0.1$  as shown in Mieske et al. (2002). *Open Stars* – faint fuzzy M31 clusters from Huxor et al. (2005). *Open Squares* – young massive clusters (YMCs) from Bastian et al. (2006). Note that Padova models suggest  $M_{F814W} \sim M_I$  to within a few hundredths of a magnitude.

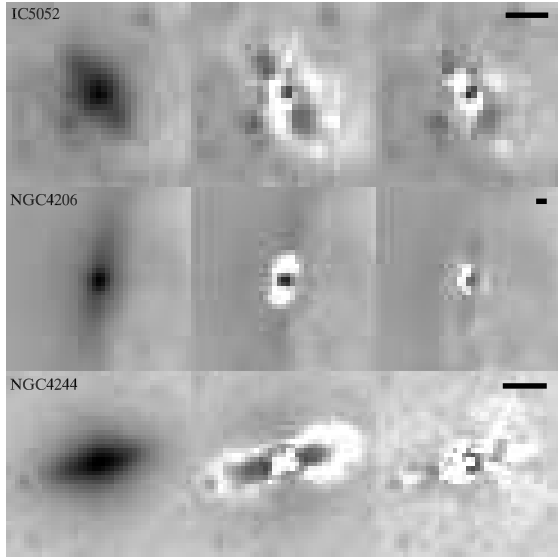


FIG. 4.— Residuals of model fits to F606W observations of nuclear clusters in IC 5052, NGC 4206, and NGC 4244. The images show the area over which fits were done, and are in the coordinate system of the ACS images. They are thus rotated from the images in Figs. 1 and 5. Bars in the upper right show a length of 10 pc in each galaxy. The left most column shows the original image, the middle and right columns show the images after subtraction of the best-fitting elliptical King and elliptical King + disk profiles. All are shown with the same scaling. In each case, the elliptical King + disk profile clearly provides a better fit to the cluster than a single-component elliptical King profile.

to those for the single-component fit (Table 2). The improvement is most dramatic in NGC 4244, and is least significant in IC 5052. However, the reduced  $\chi^2$  values remain well above unity suggesting the model doesn't fit the data perfectly. For IC 5052 and NGC 4244, the disk scale lengths are comparable to the effective radii of the spheroidal components ( $h_x \sim 3$  pc), while in NGC 4206 the disk component is very extended ( $h_x = 31$  pc).

In NGC 4206 and IC 5052, the residuals show a similar pattern which suggests the presence of a compact central source and/or a ring rather than a disk. We discuss the issue of whether the components are rings or disks in the section below. Both these galaxies also show a color-gradient perpendicular to the major axis, suggesting the presence of a thin dust disk.

### 3.1.3. Rings vs. Disks

In this section we present evidence that the flattened components in NGC 4206 and NGC 4244 clusters are better fit by a disk model than a ring model, while in IC 5052, a ring model provides a better fit. In all three cases, it appears that the disk or ring extends to small radii and overlaps with the light distribution of the spheroidal component.

In Table 4 we present the best-fitting ring + elliptical King models for each image. For the ring component, we assumed a constant midplane density with an outer ( $r_{out}$ ) and inner ( $r_{in}$ ) radius:

$$\text{if } x < r_{in} : \quad (3)$$

$$\Sigma(x, z) = 2\rho_0 \operatorname{sech}^2\left(\frac{z}{z_0}\right) \left(\sqrt{r_{out}^2 - x^2} - \sqrt{r_{in}^2 - x^2}\right)$$

if  $r_{in} < x < r_{out}$  :

$$\Sigma(x, z) = 2\rho_0 \operatorname{sech}^2\left(\frac{z}{z_0}\right) \left(\sqrt{r_{out}^2 - x^2}\right)$$

else :  $\Sigma(x, z) = 0$

This model is brightest for  $r_{in} < x < r_{out}$ , and contributes less flux near the center, making it qualitatively different from the disk model (Eq. 2). However, given that the details of both models are somewhat arbitrary, the results of the fits should be viewed with some caution.

For the NGC 4206 and NGC 4244 NCs the ring fits (Table 4) have reduced  $\chi^2$  values that are 20-75% higher than the disk values shown in Table 3. Furthermore, the best-fitting ring models have inner radii extending all the way to the center of cluster. Thus, the evidence suggests that in the NGC 4206 and NGC 4244 NCs, the second, flattened component is disk-like rather than being ring-like.

In contrast, the NC in IC 5052 shows two symmetric spots in its residuals (Fig. 4) and color map (Fig. 5). Not surprisingly, the ring model provided a better fit (20% decrease in reduced  $\chi^2$ ), with an inner and outer radius of the ring of 6.8 pc and 11.8 pc, respectively. The whole ring falls well within the tidal radius of the spheroidal component ( $\sim 24$  pc), and thus their stellar distributions appear to overlap.

Nuclear rings have previously been detected in molecular gas (e.g. Böker et al. 1997, 1998) and UV stellar light (e.g. Maoz et al. 1996). However, these studies find rings an order of magnitude larger in size than the one we find in IC 5052. The only previously observed structure around a nuclear cluster on a similar scale to the IC 5052 ring and NGC 4244 disk is the compact molecular disk detected coincident with the nuclear cluster in IC 342 (Schinnerer et al. 2003) which has a diameter of 30-55 pc depending on the assumed distance to the galaxy. We note that this disk is barely resolved by their CO observations (with a resolution of  $1.2''$ ), and may therefore be either a disk or a ring.

The evidence in all three clusters that the disk or ring components do overlap with the spheroidal components justifies our labeling these three nuclear clusters as multi-component clusters. For simplicity, and because disk models are preferred in two of the three multi-component clusters, we will refer to the flattened components in the next few sections as being disks. We will return to the formation and possible role of rings in our discussion (§7.1.3).

### 3.2. Luminosities

The F814W absolute magnitude ( $M_{F814W}$ ) and the F606W-F814W color are given in Table 1. Photometry was done using the Vega-based zeropoints and reddening coefficients from Sirianni et al. (2005). The foreground reddening was corrected using values of  $E(B-V)$  from Schlegel et al. (1998), which were at most 0.05 mags. These measurements are complicated by the high and variable background level and the complex shapes of the nuclear clusters. A scatter of  $\sim 0.1$  magnitudes was found by varying the aperture size within reasonable limits. The formal errors on the calculated magnitudes are quite small (typically  $< 0.01$  mags). Magnitudes from the fitted models agree with the aperture magnitudes in cases

TABLE 3  
ELLIPTICAL KING + DISK PROFILE FITS

Galaxy	Pix. Scale [pc/pixel]	Filter	Disk			Ell. King			$\Delta$ PA [ $^{\circ}$ ]	Reduced $\chi^2$
			$\mu_0$ [mag/ $\square''$ ]	$h_x$ [pc]	$z_0$ [pc]	$\mu_0$ [mag/ $\square''$ ]	$r_{eff}$ [pc]	$q$		
IC 5052	1.46	F606W	17.27	3.54	1.47	16.15	3.97	1.00	-10.8	20.3
IC 5052	1.46	F814W	16.28	3.48	1.19	14.74	3.55	1.00	-12.0	15.7
NGC 4206	4.39	F606W	17.44	31.00	15.76	12.87	4.94	0.45	5.1	26.8
NGC 4206	4.39	F814W	16.61	31.36	17.42	12.00	5.32	0.44	5.0	16.7
NGC 4244	1.06	F606W	13.64	2.51	1.64	16.29	10.79	0.78	-10.1	15.1
NGC 4244	1.06	F814W	13.18	2.73	1.42	13.84	5.70	0.73	-9.6	16.3

TABLE 4  
ELLIPTICAL KING + RING PROFILE FITS

Galaxy	Filter	Ring				Ell. King			$\Delta$ PA [ $^{\circ}$ ]	Reduced $\chi^2$
		$r_{out}$ [pc]	$r_{in}$ [pc]	$z_0$ [pc]	$L_{ring}/L_{tot}$	$\mu_0$ [mag/ $\square''$ ]	$r_{eff}$ [pc]	$q$		
IC 5052	F606W	11.83	6.83	1.44	0.18	15.64	3.24	1.00	-11.0	16.9
IC 5052	F814W	12.13	6.91	1.61	0.14	14.36	3.05	1.00	-11.5	13.2
NGC 4206	F606W	84.82	0.44	18.56	0.53	13.57	7.69	0.48	5.3	32.5
NGC 4206	F814W	83.78	0.44	20.69	0.53	12.59	7.70	0.47	5.2	21.5
NGC 4244	F606W	10.42	0.11	0.92	0.18	13.19	4.07	0.58	-10.1	26.7
NGC 4244	F814W	10.75	0.14	0.91	0.16	12.51	4.25	0.59	-9.7	23.5

where the data is well-fit, but differ substantially when the fits are poor.

Figure 3 plots the F814W aperture magnitudes measured for all nine nuclear candidates against their fitted half-light radius from the elliptical King profiles. We also plot magnitudes and sizes of other compact stellar systems, assuming that  $M_I \sim M_{F814W}$  since the F814W filter is very similar to the Johnson  $I$  filter, with single-stellar populations expected to be  $\sim 0.03$  magnitudes brighter in F814W than in  $I$  (Girardi 2006).

Examination of Figure 3 shows that the magnitudes and sizes of the objects in our sample are similar to the NCs found by Böker et al. (2002, 2004) (*filled circles*) for their sample of face-on, late-type galaxies. Böker et al. (2004) measure sizes for only the brighter clusters in their sample, but find NCs with measured magnitudes as faint as  $M_I = -8.6$ . Because of their galaxies' face-on orientations, clusters with disk and spheroid components such as we have observed would have gone unnoticed in their study. The morphology of the M33 nuclear cluster is flattened ( $\epsilon = 0.17$ ) along an axis parallel to the major axis of the galaxy (Lauer et al. 1998; Matthews et al. 1999), as would be expected for a multi-component cluster observed at the inclination of M33's disk. The stellar populations in the spectra of both M33's NC (Long et al. 2002) and some of the objects in the Böker et al. (2002) sample (Walcher et al. 2006), are also similar to what we see in §4.2 for NGC 4244's NC. It is therefore clear that the nuclear clusters observed here are similar to those found previously. Furthermore, the multi-component morphology may be a common feature of nuclear clusters.

We also note that the two most luminous clusters are those with the most prominent disk components (NGC 4206 & NGC 4244). This correlation is not surprising, as the disks seem to be composed of recently formed stars (see §4) and would therefore have low mass-

to-light ratios. Over time, as the young stellar populations age the disks will become less prominent.

The observed color of the clusters (see Table 1) can constrain the total dust column to the center of the host galaxies. We estimated rough lower and upper limits on the total reddening by comparing the colors of the NCs to that of an old and red, or young and blue stellar population. For most of the galaxies, the F606W-F814W NC colors of  $\sim 1$  suggest that the reddening lies between  $E(B-V)$  of 0 and 1. However, for NGC 3501 & NGC 4517 the reddening must be greater than 0.7 mags.

#### 4. NUCLEAR CLUSTER STELLAR POPULATIONS

In this section we demonstrate that the multiple structural components seen in some NCs in §3 also have distinct stellar populations. In particular, the disk components are made of younger stars than the spheroidal components. We first examine color maps of the clusters and argue that the disks most likely have populations younger than 1 Gyr. We then examine the bright nearby NC in NGC 4244 in detail, using multi-band photometry and spectroscopy (see Fig. 6) to show that the spectra is best fit by two or more epochs of star formation.

Two recent papers have presented very thorough studies of the stellar populations of nuclear clusters in both early and late type spiral galaxies (Walcher et al. 2006; Rossa et al. 2006). Both use fitting of spectra to convincingly show that nuclear clusters contain multiple generations of stars. For a sample of nine bright nuclear clusters in late-type galaxies, Walcher et al. (2006) has shown that all of the clusters observed had stellar populations younger than 100 Myr. The typical mass of the youngest stars was a few  $\times 10^5 M_{\odot}$ . However, in most of the clusters, the bulk of the stellar mass had an age of  $\gtrsim 2.5$  Gyr. Our findings on the stellar populations in our multi-component clusters, presented below, are fully consistent with these papers.

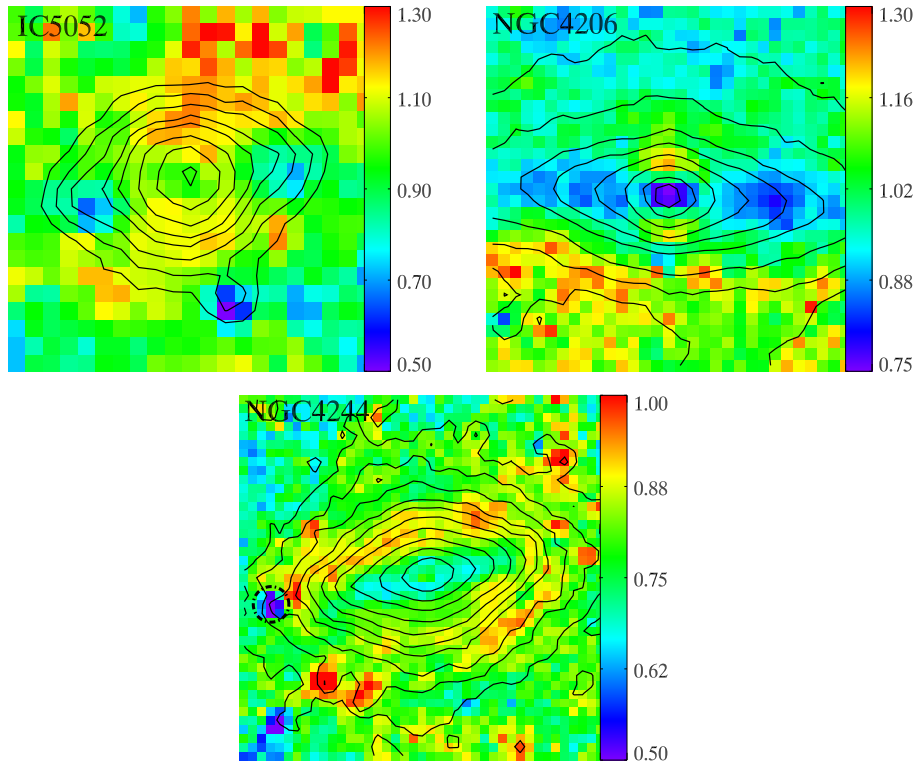


FIG. 5.— Maps of the F606W-F814W [VEGAMag] color for each cluster. Contours showing the F606W brightness are overlaid in black. The clusters with obvious disk components (IC 5052, NGC 4206, & NGC 4244) all show bluer disks and redder spheroids. The color bars on the right side indicate values for the F606W-F814W color. Colors have been corrected for foreground reddening. The central eight pixels of the NGC 4244 NC were saturated and thus don't give accurate colors. The circled region in NGC 4244 shows the suspected HII region used to obtain a dynamical mass estimate in §5.

#### 4.1. Color Maps

Figure 5 shows F606W-F814W color maps for the three nuclear cluster candidates identified as having multiple components. In each cluster, an obvious and significant color difference exists between the disk and spheroidal components. The disks are 0.3-0.6 magnitudes bluer in F606W-F814W than the reddest parts of the spheroids.

The observed color difference between the disk and spheroid components is most simply interpreted as a difference in stellar population. Despite the unknown reddening, we can place upper limits on the age of the disk component. Using the Padova single stellar population models (Girardi 2006), for a 10 Gyr old stellar population with metallicities between  $[\text{Fe}/\text{H}]$  of -1.7 and -0.4, the F606W-F814W color ranges from 0.73 to 0.91, with redder colors for more metal-rich populations. The difference in color between a 10 Gyr and 1 Gyr population is  $\lesssim 0.25$  magnitudes regardless of metallicity, suggesting that disks cannot be composed solely of intermediate age ( $>1$  Gyr) stars. At ages younger than 1 Gyr, however, the color quickly becomes bluer. Thus the  $> 0.3$  mag color difference is evidence that the disks have stellar populations younger than 1 Gyr. Put another way, we find that the disk components all must have intrinsic colors bluer than  $F606W-F814W=0.65$ , which corresponds to single-stellar populations younger than 1 Gyr. Our analysis of the spectrum of NGC 4244's NC (§4.2) confirms that stars with ages  $\lesssim 100$  Myr are present. Furthermore, each of the nine nuclear cluster spectra ana-

lyzed by Walcher et al. (2006) showed evidence for stellar populations with ages  $< 100$  Myr

The suggested interpretation of the color difference as a difference in stellar population may be complicated by a number of factors. First, even if two separate components exist, both likely contribute to the observed color at most locations. This overlap suggests that the actual spread in age is larger than implied by the color differences. Second, the colors could be affected by the presence of dust structures on the same scale as the clusters or by emission line contribution. Based on the symmetry of the nuclear clusters (e.g. the disk is roughly the same color on both sides of the nucleus), and the spectral results from §4.2 we believe that the color difference is unlikely to be due solely to dust or emission lines and instead really does reflect a difference in stellar population.

#### 4.2. Stellar Populations in NGC 4244

In the previous section we showed that the color offset between the disk and spheroid components of the nuclear cluster indicates that the disk has a systematically younger stellar population. However because of the uncertain reddening, the ACS colors alone cannot accurately constrain the ages of the stellar populations. In this section we use our APO spectrum and photometry of the NC in NGC 4244 from the Sloan Digital Sky Survey (SDSS) and 2MASS survey to constrain the cluster's age. Before describing the details of this analysis we first describe the photometry.

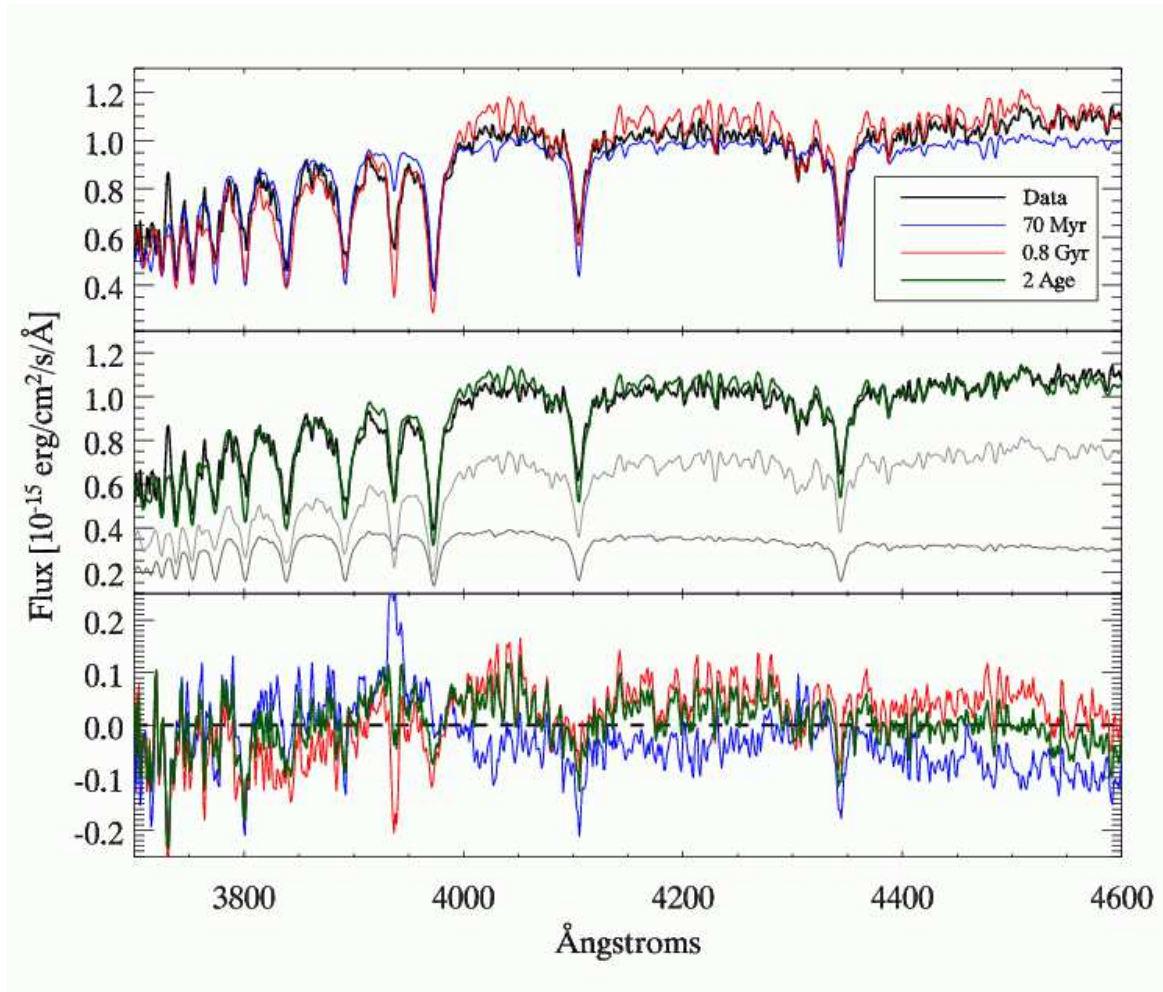


FIG. 6.— A portion of the APO/DIS spectrum of the NGC 4244 NC with best-fitting models overplotted. Only the portion of the spectrum with the most significant spectral features are shown. *Top Panel* – single-age best fits at 70 Myr and 0.8 Gyr – the ages at which there are minima in the joint- $\chi^2$  distribution (see Fig. 7). The most age-sensitive portion of the spectrum lies around the Ca H line at  $\sim 3940\text{\AA}$ , although numerous other features also cannot be fit well with a single-age population. *Middle Panel* – the best two-age fit, including both stars with ages of 0.1 Gyr (dark gray line) and 1.0 Gyr (light gray line). This fit is a significant improvement relative to either single-age fit. *Bottom Panel* – Residuals for all three fits.

The nuclear cluster in NGC 4244 is prominent, and stands well above the emission from the galaxy disk. Because of this, it was detected as a point source in both the SDSS and 2MASS surveys. This data complements the spectroscopic data by giving a large wavelength baseline to constrain the mass, reddening, and ages of the NC (de Grijs et al. 2003). In both surveys, the source is essentially unresolved, and photometry is determined from PSF-fitting. In the SDSS survey, the DR4 object ID is 58773909806344622, with PSF magnitudes of 17.81, 16.62, 16.18, 15.96, and 15.73 in the  $u'$ ,  $g'$ ,  $r'$ ,  $i'$ , and  $z'$  filters. In 2MASS, the object ID is 12172945+3748264, with magnitudes of 14.36, 13.75, and 13.55 in  $J$ ,  $H$ , and  $K$  bands. The errors on the SDSS magnitudes are  $\sim 0.02$  mags, while the 2MASS observations have errors of  $\sim 0.05$  mags. The difference in resolution and photometric methods between the two surveys means there may be some relative systematic error in the magnitudes. Therefore, any conclusions based on the photometry alone should be considered with caution. We note that because the central pixels of the NC were

saturated in the ACS data (taken with gain=1  $e^-$ ), we were unable to derive accurate photometry from the HST images.

#### 4.2.1. Single-Age Fits

In principle, the photometry and spectrum can be fit with arbitrary stellar populations, but in practice this leads to far too many degeneracies. To simplify the problem we started by assuming the NGC 4244 cluster contains stars of a single age and then determine a best-fitting extinction, mass and  $\chi^2$  as a function of age from both the photometric and spectroscopic data separately. For the photometric data, we used the single-stellar population models from the Padova group (Girardi et al. 2004) using the Marigo (2001) treatment of the AGB. These models have been produced for both the SDSS and 2MASS photometric systems and assume a Kroupa (2001) initial mass function (IMF) between 0.1 and 100  $M_{\odot}$ . The extinction was calculated in  $A_v$  assuming  $R_v = 3.1$  using coefficients from Girardi et al. (2004) and Cardelli et al. (1989) for the Sloan and 2MASS data respectively. For the spectroscopic fitting, single stellar

population spectral templates from Bruzual & Charlot (2003) were used. These templates assume a Chabrier (2003) IMF from 0.1 to  $100 M_{\odot}$ . They have  $1\text{\AA}$  resolution, and were redshifted and interpolated to the wavelengths of our observed spectrum. The reddening was applied to the spectrum using the Cardelli et al. (1989) prescription. We fit the feature rich blue side of the DIS spectrum extending from  $3650\text{\AA}$  to  $5500\text{\AA}$  which contains Balmer, He I, Mg, and Ca H & K lines (see Fig. 6). The signal-to-noise of this portion of the spectrum ranged from 20 to 60. For both the photometry and spectroscopy, we determined the best-fitting mass and reddening at a given age using the IDL CURVEFIT routine. All fits were done assuming a distance modulus of 28.20 ( $D=4.4$  Mpc, Seth et al. 2005), and a metallicity of  $[\text{Fe}/\text{H}]=-0.4$ , similar to the expected current gas phase metallicity of NGC 4244 (Garnett 2002). This is the same metallicity derived from composite age fits for a majority of the clusters found by Walcher et al. (2006). Furthermore, Rossa et al. (2006) and Walcher et al. (2006) have shown that the inferred age distribution does not depend strongly on the metallicity.

Figure 7 shows the results of our fits for single stellar populations with ages between  $10^7$  and  $10^{10}$  years for both the spectroscopy and photometry. The top panel indicates the  $\chi^2$  of the best-fitting model at each age. The spectrum is best fit by populations younger than  $\lesssim 10^9$  years, stellar masses of  $2\text{--}3 \times 10^6 M_{\odot}$  and decreasing extinction with increasing age. The  $\chi^2$  has a minimum at ages of  $\sim 0.8\text{--}1.0 \times 10^9$  years (just before the onset of the RGB), and then increases rapidly towards older ages. This results from the template spectrum becoming redder than the observed spectrum. A shallower  $\chi^2$  minima is also seen in the spectra at  $\sim 50\text{--}100$  Myr.

The fits to the photometric data have two comparable  $\chi^2$  minima at  $\sim 10^8$  and  $\sim 10^9$  years, with the younger age being somewhat preferred. The minima at these two ages is more pronounced in the photometric data than in the spectroscopic data, perhaps as a result of the photometric data's longer wavelength coverage. Combining the photometric and spectroscopic results, the minima in the joint  $\chi^2$  are at 70 Myr and 0.8 Gyr. The masses from the photometric data at these minima are  $3\text{--}5 \times 10^6 M_{\odot}$ , somewhat more massive than the spectral data. This difference may result from light lost outside the  $1.5''$  wide slit, uncertainty in the absolute calibration of the spectroscopic data, and/or differences in the assumed IMF.

Spectral fits from the two joint- $\chi^2$  minima are shown in Figure 6. The younger age appears to fit the bluer part of the spectrum better, while the older age more accurately fits many of the lines and the redder continuum. The Ca H line is particularly age sensitive, being much too shallow in the younger age and too deep in the older age.

#### 4.2.2. Multi-Age Fits

The color difference between the disk and spheroid components discussed in §4.1 and the recent results of Rossa et al. (2006) and Walcher et al. (2006) strongly suggest that NCs contain stellar populations of multiple ages rather than the single-age populations assumed above. We have tried to constrain the ages and masses of the multiple stellar populations in NGC 4244's NC in two ways: (1) by fitting a weighted average of two or three stellar populations of different ages to the spec-

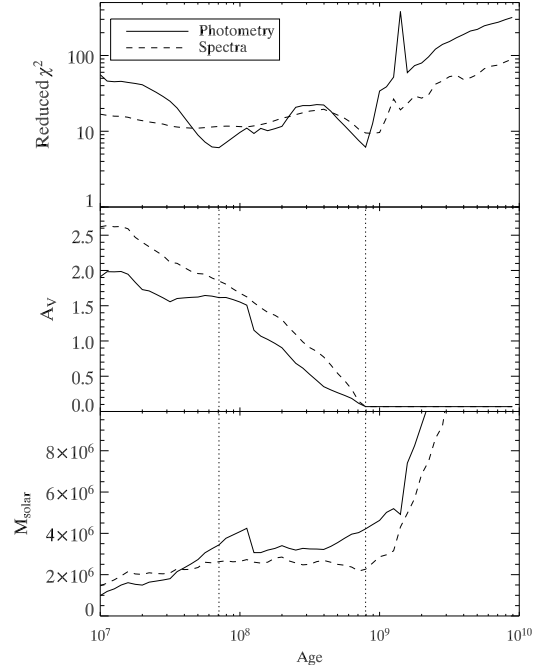


FIG. 7.— Photometric and spectroscopic fits of the mass and reddening of the NGC 4244 NC using single-stellar population models. *Top panel* – the reduced  $\chi^2$  values of the best-fitting mass and reddening at each age. *Middle panel* – The best-fitting reddening, *bottom panel* – the best fitting mass. The dashed vertical lines indicate the two minima in the joint  $\chi^2$  distribution at 70 Myr and 0.8 Gyr.

tral and photometric data, or (2) by fitting the spectrum to a constant star formation rate (SFR) model from Bruzual & Charlot (2003). These approaches both give significantly better fits to the data than single-stellar population models, reducing  $\chi^2$  values by 50% or more. However, it is also clear that there is no unique solution; *the data can be fit equally well by many different combinations of stellar populations and reddening values*. Note that we assumed a single extinction ( $A_V$ ) value for all components.

Of the nine NC spectra presented in Walcher et al. (2006), our spectrum of the NGC 4244 NC most closely resembles their spectrum of the NGC 7793 NC. From their fits to composite stellar populations, they find that the NGC 7793 cluster has an average stellar age of  $\sim 2$  Gyr, but has young stars ( $\lesssim 100$  Myr) that make up 10% of the mass. This is qualitatively similar to what we find below for the NGC 4244 NC.

*Two Age Models:* The simplest stellar population model consistent with the color maps is a two-age stellar population: a young population associated with the disk, and an older population associated with the spheroid. Taking the two minima seen in the single-stellar population fits at ages of 70 Myr and 0.8 Gyr as a starting point, we explored what combination of two populations gives the best fit to both the spectroscopic and photometric data. For a young component with ages between 50-100 Myr and an intermediate-age component with ages between 0.6 and 1.0 Gyr, the best fits to the spectroscopy have  $A_V \sim 0.5$ , masses of  $0.5\text{--}3 \times 10^5 M_{\odot}$  for the young

stellar population, total masses of  $2\text{--}4 \times 10^6 M_{\odot}$ , and reduced  $\chi^2$  values of  $\sim 6$ . However, for the photometry, the best fits favor an  $A_V > 1$  and masses dominated by the young component. These photometric fits clearly do not reproduce the shape or lines in the spectra, thus we restricted ourselves to lower  $A_V$  solutions. When  $A_V$  is restricted to be less than one, the photometric fits are in relatively good agreement with the spectroscopic fits. However, the implied stellar masses for both the young and intermediate-age components are up to two times larger than the spectroscopic best-fit models, similar to what was seen in the single-age fits. Overall, we find that ages of 0.1 and 1.0 Gyr do the best job of matching both sets of data. The spectroscopic best fit at these ages is shown in Figure 6, and has  $A_V = 0.46$ ,  $1.9 \times 10^5 M_{\odot}$  of 0.1 Gyr old stars and  $3.1 \times 10^6 M_{\odot}$  of 1 Gyr old stars.

Based on the color map of the nuclear cluster, we expect the younger stellar component in the two-age fits be associated with the disk. We can test the consistency of this idea by comparing our spectral fits to the luminosities of the disk component decomposed from the HST data in §3. Assuming that the disk is dominated by  $\sim 70$  Myr old stars, the expected F606W-F814W color from the Padova models is 0.25 (Girardi 2006). The observed disk component color is 0.4, requiring an extinction  $A_V = 0.47$  mags. Using this extinction and mass-to-light ratios from the Padova models, we derive a mass for the disk component of  $1.2 \times 10^5 M_{\odot}$ . *Both the mass and extinction derived from the luminosities of the disk component in the HST data agree with the young stellar mass and extinction determined in the two-age spectral fits.* This agreement strongly suggests a link between the blue disk component and the young stellar component that appears to be required to fit the blue spectral features.

*Three Age Models:* We also explored the sensitivity of our fits to the inclusion of a third, old (10 Gyr) stellar population. We find that a large mass of old stars is consistent with both the photometric and spectroscopic data. Best-fits to both data sets have low  $A_V$  ( $< 0.4$ ), total masses of  $\sim 10^7 M_{\odot}$  with 90% of that mass in the old component, and  $\sim 10^5 M_{\odot}$  in the young component, similar to the two-age fits. The inclusion of the older component significantly improves the photometric fit to the data (reduced  $\chi^2 = 1.7$ ), suggesting older stars may indeed be present. However, the spectral fit is insensitive to this old component; the best-fit spectrum is nearly identical to the two-age fits, despite 90% of the mass being contained in the old component.

The effects of disk contamination on the photometry and spectra should be minimal given the prominence of the NGC 4244 NC. Furthermore, by comparing HST/STIS and ground-based spectra, Walcher et al. (2006) show that the stellar population immediately surrounding the nuclear cluster in late-type galaxies seems to have a population similar to the cluster itself. Both Rossa et al. (2006) and Walcher et al. (2006) find some evidence for an underlying old stellar component in many of their nuclear cluster spectra. We note that all the masses quoted here refer to the *initial* mass in stars required to fit the current spectral data. Due to stellar evolution, the current mass of a cluster dominated by old stars would be  $\sim 2 \times$  lower than the initial mass, given reasonable initial mass functions.

*Constant SFR model:* Using the Bruzual & Charlot (2003) codes, we generated a model spectrum assuming a constant SFR from 12 Gyr to the present. The best-fit of this model to the data gives a current mass of the cluster of  $6.2 \times 10^6 M_{\odot}$ , and a reddening of  $A_V = 0.72$ . The reduced  $\chi^2$  of the fit is 5.7, within 10% of the reduced  $\chi^2$  of the best fits obtained for the two- and three-age models. The spectral shape of the constant SFR model appears to be somewhat redder than the data, suggesting either the need for relatively more young stars than in the constant SFR model, or for a more realistic metallicity evolution, in which the older stars are bluer and more metal-poor. The former point is supported by Walcher et al. (2006), who have shown that in their sample of clusters, the star formation rate in the past 100 Myr is an order of magnitude greater than the star formation rate between 0.3 and 20 Gyr. However, this enhancement of recent star formation may result from a bias in their sample towards brighter nuclear clusters.

#### 4.2.3. Summary of Stellar Populations in the NGC 4244 NC

We draw the following conclusions from the spectral and photometric fits of the NGC 4244 NC:

1. Multiple stellar populations definitely provide improved fits over single-stellar populations for both the spectroscopy and photometry of the NGC 4244 NC. However, many different combinations of masses and ages fit the data well.
  2. The best-fitting single stellar populations have ages of either  $\sim 70$  Myr or  $\sim 0.8$  Gyr.
  3. The total current mass of the cluster appears to be between  $0.2$  and  $1 \times 10^7 M_{\odot}$ .
  4. If we assume only two ages are present, the youngest ( $\lesssim 100$  Myr) stellar component appears to have  $\sim 10^5 M_{\odot}$  of stars. This mass is consistent with the luminosity of the disk component decomposed using the morphological fits in §3.
  5. For all multi-age fits, the mass of stars younger than 100 Myr is a small fraction ( $< 5\%$ ) of the total mass of the cluster.
  6. Stars older than 1 Gyr may be present in large numbers ( $\sim 10^7 M_{\odot}$ ). Inclusion of an old stellar population particularly improves our fits to the SDSS and 2MASS photometric data.
  7. A constant SFR fits the data as well as assuming two or three discrete ages.
5. A DYNAMICAL MASS ESTIMATE FOR THE NGC 4244 CLUSTER

Emission lines, including  $H\alpha$ , [NII], [SII], and [OII] are seen in our spectrum of the NGC 4244 NC. For the  $H\alpha$  line, the emission component is redshifted relative to the underlying stellar absorption lines (see Fig. 8). We utilize this offset between the emission and absorption components to obtain a dynamical mass estimate for the NGC 4244 cluster.

Examination of the color map for NGC 4244 in Figure 5 shows a very blue compact source located along

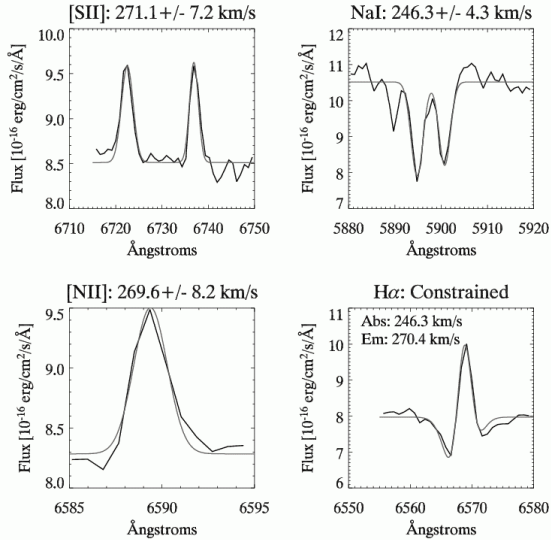


FIG. 8.— Spectral lines used to derive the relative offset between emission and absorption. Dark lines show the actual spectrum, while lighter lines show the best fitting gaussian or double-gaussian model. The number in the title of each panel gives the fitted velocity and error bar. The spectra has a  $S/N \sim 35/\text{pixel}$ .

the NC plane on the left (NE) side,  $0.88''$  (18.6 pc projected) from the NC center. This compact blue object has an F606W-F814W color of  $\sim 0.3$ , which is  $\sim 0.4$ - $0.6$  mags bluer than the disk and spheroid components of the cluster. Assuming moderate reddening and blending with the outer isophotes of the cluster, the color of the blue knot is consistent with this object being an HII region. HII regions in our filter combination appear very blue because there are strong emission lines located in the F606W filter and not in the F814W filter. Measurements of HII regions in NGC 55 (the nearest galaxy in our sample) suggests HII regions have typical colors of F606W-F814W =  $-0.2$  with a  $\sim 0.2$  mag scatter.

This likely HII region falls within the slit used for our nuclear cluster spectrum. Therefore, we identified this object as the likely source of the emission lines in our spectra. We verified this by extracting spectra from the left (NE) and right (SW) sides of the cluster. The left side spectrum shows significantly enhanced emission lines relative to the right side. However, because the seeing was  $\sim 1''$ , we were unable to spatially separate the emission component from the nuclear cluster. We now proceed under the assumption that the emission lines in our spectrum are associated with this compact blue object.

To determine the relative velocity of the emission and absorption components we fit the [SII] doublet and [NII] line to determine the emission line velocity, and fit the NaI doublet to determine the absorption line velocity. We obtained a weighted mean velocity of  $270.5 \pm 5.4$  km/sec for the emission lines and  $246.3 \pm 4.3$  km/sec for the NaI absorption line assuming air wavelengths for the lines from the Atomic Line List<sup>1</sup>. This absorption velocity matches the systemic velocity of NGC 4244 ( $244.4 \pm 0.3$  km/sec, Olling 1996) to within the error bars, as would be expected for the nuclear cluster. We note that this HII region is counter-rotating with respect to

the galaxy disk.

Figure 8 shows the fitted emission and absorption lines, as well as the best fit of absorption + emission for the H $\alpha$  line after fixing the velocities of the absorption and emission to the values derived from the NaI, [SII], and [NII] lines. This H $\alpha$  line fit does a good job of replicating the observed line shape thereby suggesting that the velocities we have derived are correct.

Assuming the projected radius of the HII region is close to the true radius, and that it is bound to the NGC 4244 NC nuclear cluster, the  $\Delta v = 24.1 \pm 7.0$  km/sec offset between emission and absorption implies a nuclear cluster mass of  $2.5^{+1.7}_{-1.2} \times 10^6 M_{\odot}$  within a radius of 19 pc. If the object is indeed rotating around the cluster, but is in front of or behind the cluster (thus making its projected distance larger), then the mass we derived is a lower limit on the mass of the cluster.

This rough estimate of the dynamical mass of NGC 4244's NC is consistent with the stellar masses determined for the one- and two-age fits in §4.2. It is also consistent with the constant SFR or three-age model fits ( $M \sim 6 \times 10^6 M_{\odot}$ ) if the HII region is seen in projection and lies  $\sim 25$  pc from the center of the nuclear cluster.

The estimated mass is also similar to the typical mass determined by Walcher et al. (2005) for late-type galaxy nuclei. They derived masses for nine nuclear clusters from the Böker et al. (2002) sample by combining size and velocity dispersion measurements. Their total range of masses is  $8 \times 10^5 M_{\odot}$  to  $6 \times 10^7 M_{\odot}$ , with seven of the nine clusters having masses between  $0.1$  and  $1 \times 10^7 M_{\odot}$ . We note that they have determined these masses assuming spherical symmetry; if these clusters have disk components similar to the ones we have observed here, the masses derived by Walcher et al. (2005) may be underestimated, since they do not take into account the rotational support that would be expected in a disk. Given that their clusters contain young stellar populations (Walcher et al. 2006), this effect could be significant.

## 6. NGC 4206: POSSIBLE INDICATION OF AN AGN COMPONENT

In this section, we present evidence that the nuclear cluster in NGC 4206 may contain an AGN component. This evidence is very tentative and requires confirmation with follow-up observations.

An SDSS spectrum (MJD 53149, Plate 1612, Fiber 603) exists for the central regions of NGC 4206. Due to the  $3''$  diameter ( $\sim 250$  pc) aperture, this spectrum is dominated by the light from the central regions of the galaxy and not by the nuclear cluster. In addition to a dominant old stellar spectrum, narrow H $\alpha$ , [NII], and [SII] emission are clearly seen. No broad emission lines are seen. Examining the HST color map, the center of the nuclear cluster is the bluest area anywhere within the SDSS spectral aperture. Since emission line sources are very blue in our filter combination, the central portion of the nuclear cluster is the likely source of the emission lines. The emission lines are not offset in velocity from the absorption spectrum (as was seen in NGC 4244) further supporting their nuclear origin.

The ionizing source of the observed emission lines could be either star formation or AGN activity at the center of the nuclear cluster. These two ionizing sources can be

<sup>1</sup> <http://www.pa.uky.edu/~peter/atomic/>

distinguished using the line ratio of [NII] and H $\alpha$ . Because the H $\alpha$  line is contaminated by stellar absorption, we model the underlying stellar continuum with a single stellar population  $\sim 3$  Gyr in age with  $A_V \sim 0.5$ . After subtracting this spectrum, the line ratio of the remaining emission lines is  $\log([\text{NII}]/\text{H}\alpha) \sim -0.3$ . Based on the recent analysis of SDSS spectra by (Obric et al. 2006), this line ratio suggests that the source is a “mixed” starburst/AGN. NGC 4206 may therefore host a small AGN within the core of the nuclear star cluster. If confirmed by follow-up observations, this would make it only the second late-type spiral known to have both a SMBH and massive nuclear star cluster, the other being NGC 4395, an Sd galaxy with  $M_B \sim -17.5$  hosting a nuclear cluster with  $M_I \sim -10.1$  (Matthews et al. 1999), and a black hole with a mass of  $\sim 10^4 - 10^5 M_\odot$  (Filippenko & Ho 2003). In earlier type spirals, other examples exist of the co-existence of nuclear star clusters and AGN (e.g. Thatte et al. 1997; Davies et al. 2006). We plan to test for the presence of AGN components in all of our multi-component nuclear cluster candidates with near-IR integral field unit spectroscopy using adaptive optics.

## 7. DISCUSSION

We now discuss how our data constrains the formation mechanisms of nuclear clusters. We suggest a formation mechanism in which stars in nuclear clusters form episodically in disks and then over time lose angular momentum or are heated vertically, ending up in a more spheroidal distribution. After discussing this mechanism in some detail, we examine the relation of nuclear clusters to other massive star clusters and supermassive black holes.

### 7.1. Formation Mechanisms

Our observations of multi-component clusters place significant constraints on nuclear cluster formation mechanisms. The presence of young NC disks ( $< 1$  Gyr) aligned with the disks of the host galaxies strongly suggests that they are formed *in situ* from gas accreted into the nuclear regions. We have shown in §3.2 that these disks may be a common feature of nuclear clusters. Such disks cannot be formed via the accretion of globular clusters by dynamical friction. While globular cluster accretion very likely occurs, this mechanism has been shown to be relatively inefficient in late-type galaxies (Milosavljević 2004). We propose here a scenario in which the *dominant* formation mechanism for nuclear clusters is via *in situ* formation in disks. Although the mechanism will need to be tested with detailed simulations, it is consistent not just with our data, but with both the evidence for young and composite stellar populations in many nuclear clusters (e.g. Walcher et al. 2006), and the direct detection of a molecular gas disk coincident with the nuclear cluster in IC 342 (Schinnerer et al. 2003).

On a large scale ( $\sim 1$  kpc), both dissipative merging of molecular clouds and magnetorotational instabilities have been shown to be capable of supplying the nucleus of a late-type galaxy with sufficient gas to form nuclear clusters (Milosavljević 2004; Bekki et al. 2006). Our proposed *in situ* formation mechanism is concerned with what occurs once the gas reaches the center. Our model is also fully consistent with the suggestion by

Walcher et al. (2006) that an initial seed star cluster is required for subsequent nuclear star cluster formation.

The details of an *in situ* formation mechanism can be constrained by our observations. To explain presence of redder/older spheroids in the multi-component clusters and the absence of disk components in a majority of our nuclear clusters, we propose a model in which nuclear cluster disks form episodically and are transformed into a rounder distribution over time due to loss of angular momentum or dynamical heating. There are two important timescales in this model: (1) the period of time between star formation episodes, and (2) the time it takes stars in a disk morphology to end up in a spheroidal distribution. We examine these two timescales in detail below.

#### 7.1.1. Period Between Star Formation Episodes

A number of authors have previously suggested that star formation in the nuclear regions of late-type spirals may be episodic. The physical motivation for episodic star formation is that a massive star formation event will feedback on the local environment preventing star formation for the next  $\sim 10^8$  years (Milosavljević 2004). Although this feedback may destroy the gas disk and shut off star formation, it does not disrupt the disk of recently formed stars, whose lifetime we discuss below in 7.1.2.

Assuming that the present epoch is not a special time in the life of the nuclear clusters, one can estimate the period on which star formation recurs. Observationally, Davidge & Courteau (2002) argue for a period of  $\sim 0.3$  Gyr based on the detection frequency of Pa $\alpha$  emission in galaxy nuclei. Schinnerer et al. (2003) also determine a recurrence period of a few hundred Myr to 1 Gyr based on the gas accretion rates observed in IC 342’s nucleus. More recently, from analysis of the youngest stellar components in the spectrum, Walcher et al. (2006) has found the typical time between star formation bursts to be  $\sim 70$  Myr with a typical mass of roughly  $1.6 \times 10^5 M_\odot$ .

Our observations of the NGC 4244 nuclear cluster are consistent with these previous estimates. Based on the  $\sim 10^5 M_\odot$  of stars in the young component (§4.2), approximately 25 episodes of disk formation must have occurred to build up the  $2.5 \times 10^6 M_\odot$  of the cluster (§5). If this occurs over a Hubble time, then the period between bursts is  $\sim 0.5$  Gyr.

#### 7.1.2. Timescale of Disk Transformation

Given that nuclear cluster disks are observed in  $< 50\%$  of nuclear clusters, and that these disks all have stellar populations younger than a Gyr, a mechanism must exist that destroys or disrupts this disk on a timescale shorter than  $\sim 1$  Gyr. We suggest that angular momentum loss or dynamical heating causes the disks to be transformed over time, thus creating the more spheroidal, older components seen in our nuclear clusters. Although mechanisms of angular momentum loss have not been studied previously in nuclear clusters, these objects are dynamically similar to globular clusters, for which the theory of rotation and rotational evolution has been well-developed (Agekian 1958; King 1961; Shapiro & Marchant 1976; Fall & Frenk 1985; Davoust & Prugniel 1990; Longaretti & Lagoute 1997).

As they age, star clusters flattened due to rotation will become increasingly round due to the preferential

evaporation of high angular momentum stars (Agekian 1958). We can compare the timescale of this angular momentum loss to the expected lifetimes of our disks. The timescale over which the ellipticity of a rotating stellar cluster decreases is  $\gtrsim 40\times$  the median relaxation time,  $\tau_{rh}$  (Shapiro & Marchant 1976; Fall & Frenk 1985). For globular clusters in the Milky Way,  $\tau_{rh}$  is typically  $\sim 10^8$  years. However, this timescale is longer for more massive clusters like  $\omega$  Cen, with  $\tau_{rh} = 3.5$  Gyr (Shapiro & Marchant 1976). For the NGC 4244 NC we have calculated a median relaxation time for the whole cluster of  $\sim 2$  Gyr (Eq. 8-72 Binney & Tremaine 1987). For just the disk component, assuming it has a mass of  $\sim 10^5 M_\odot$  and a half mass radius of  $\sim 3$  pc, we get  $\tau_{rh} = 4 \times 10^8$  years. These relaxation times suggest that the timescale for evaporation of angular momentum in NGC 4244 is in the range of 16-80 Gyr. This timescale is significantly longer than the 100s of Myrs over which we expect the disk to be transformed into a spheroidal component.

It therefore appears that angular momentum loss due to processes internal to the clusters are unlikely to transform the disk components into spheroids on sufficiently short timescales. Instead, we must look to external processes that can affect the dynamical evolution of the nuclear cluster. We have identified a few alternative mechanisms for transforming the stellar disk component into a spheroid. These include: (1) small angular offsets of the nuclear disk from the plane of the galaxy, and (2) slight positional offsets of the cluster from the center of the galaxy potential, (3) torques on the stellar disk from successive gas accretion. A forthcoming paper will discuss this problem in more detail.

### 7.1.3. Rings

We have been assuming thus far that stars are formed initially in disks, as suggested by our observations of NGC 4244 and NGC 4206. However, in §3.1.3, we showed that one of the three multi-component NCs, in IC 5052, was best fit by a spheroid + ring model with inner and outer ring radii of 6.8 and 11.8 pc. We discuss here how such a ring could form and examine rings in context of our proposed nuclear cluster formation model.

Based on an elongated near-infrared component in IC 342, Böker et al. (1997) suggested that the observed molecular ring (with radius<sup>2</sup> of  $\sim 65$  pc) results from an inner Lindblad resonances (ILR) with a stellar bar. If a similar mechanism is at work in forming the ring in IC 5052, it would require the star cluster itself to have a barred disk morphology. From HST imaging of nuclear clusters in face-on spirals, there is no evidence for bars on these scales (Böker et al. 2004). A ring could also result from tidal stripping of an infalling molecular cloud or star cluster. Assuming a pre-existing cluster with mass of  $3 \times 10^6 M_\odot$  and a  $10^5 M_\odot$  molecular cloud, the molecular cloud would be tidally stripped between radii of 8 and 20 pc for molecular cloud number densities ranging between  $5 \times 10^4$  and  $5 \times 10^3 \text{ cm}^{-3}$ . Thus, tidal stripping of a molecular cloud is a feasible mechanism for creating a ring such as the one in IC 5052.

Episodic star formation occurring at least occasionally

in rings is consistent with the proposed formation model. The ring in IC 5052 is internal to the cluster itself, so after loss of angular momentum or dynamical heating, its stars would still contribute to the stellar distribution of the spheroid. The radius of the ring depends on the current mass of the star cluster in both mechanisms for ring formation described above. This correlation might provide a natural explanation for the clear correlation of nuclear cluster size and luminosity observed in dwarf elliptical galaxies by Côté et al. (2006). A similar explanation could work for formation in disks if the size of the disks depends on the mass of the nuclear cluster. Detailed modelling of disk/ring formation and dissipation would be required to test the feasibility of this idea.

### 7.1.4. Other Formation Scenarios

Our proposed scenario naturally explains the formation of multi-component clusters. However other scenarios may also be consistent with our observations. While our observations seem to require some *in situ* formation to explain the presence of young stellar disks, they do not rule out the possibility that the multi-component nuclear clusters were formed in part from the merging of globular clusters (e.g. Tremaine et al. 1975; Lotz et al. 2001). In this “hybrid” scenario, the young disk components may be a late-time veneer on an already massive cluster formed from merged globular clusters. However, we note that Milosavljević (2004) has calculated that the timescale for dynamical friction in late-type spirals is  $\gtrsim 3 \times 10^9$  years even for relatively massive clusters ( $10^6 M_\odot$ ) located within the central kpc of the galaxy. This quantity increases for less massive and more distant clusters. He concludes that this timescale is thus too long to be the dominant mechanism for nuclear cluster formation, and shows that magnetorotational instabilities can transport sufficient quantities of gas into the galaxy center to account for the observed NCs in late-type spirals.

### 7.2. Relationship to Other Massive Star Clusters

Our observations have implications beyond just the formation of nuclear star clusters in late-type galaxies. We briefly review here the possible connections between late-type spiral nuclei and dwarf elliptical nuclei, and the evidence that some massive globular clusters and ultra-compact dwarfs are stripped nuclear clusters.

#### 7.2.1. The relation between spiral and dE nuclei

The recent study by Côté et al. (2006) shows that the nuclei of dE and late-type spiral galaxies have comparable sizes, luminosities, and frequencies of detection (see also Fig. 3). They argue that this similarity suggests a nuclear cluster formation mechanism that does not depend strongly on galaxy properties. However, the formation scenario suggested by our observations for nuclear clusters in late-type galaxies cannot take place in the gas-free dE galaxies. We therefore interpret the similarity of the nuclei in these galaxies as support for dE galaxies evolving from low-mass spiral and irregular galaxies (e.g. Davies & Phillipps 1988). In this scenario, a dE,N galaxy would result from a nucleated late-type spiral galaxy after depletion of gas through star formation or galaxy harassment (Moore et al. 1996). If so, then the ages of the nuclear clusters in dE galaxies can constrain the epoch when these systems were stripped.

<sup>2</sup> The radius of their ring was recalculated assuming the Cepheid distance to IC 342 of 3.3 Mpc derived by Saha et al. (2002).

### 7.2.2. Massive star clusters as stripped galaxy nuclei

There is direct evidence that some massive globular clusters are associated with stripped galaxies. The galactic globular cluster M54 appears to be the nucleus of the Sag dSph (Layden & Sarajedini 2000), and six of the most massive globular clusters in NGC 5128 appear to be surrounded by extratidal light (Harris et al. 2002; Martini & Ho 2004).

Stripped nuclear clusters have also been invoked to explain the multiple stellar populations observed in the most massive nearby globular clusters (e.g Gnedin et al. 2002). These observations include the large metallicity spread (Smith 2004) and double main-sequence (Bedin et al. 2004) in  $\omega$  Cen, and the spread in red giant branch colors for G1 in Andromeda (Meylan et al. 2001). More recently, Harris et al. (2006) have observed a trend towards redder colors with increasing luminosity for the brightest blue globular clusters in massive elliptical galaxies. This trend is interpreted as evidence for self-enrichment in these clusters pointing to an extended star formation history more typical of nuclear clusters than globular clusters. A similar redward trend is seen for dE nuclei by Côté et al. (2006). Self-enrichment is naturally explained in an *in situ* formation mechanism, but is not easily explained if these clusters are formed by merging less massive clusters via dynamical friction.

The ultracompact dwarf galaxies recently found in the Fornax (Phillipps et al. 2001; Drinkwater et al. 2003) and Virgo (Jones et al. 2006) clusters may also be related to nuclear star clusters. One possible mechanism for their formation is “galaxy threshing”, in which nucleated galaxies lose their envelopes leaving behind only their nuclei as UCDs (Bekki et al. 2001). In the  $M_I$  vs.  $\log(r_{eff})$  diagram in Figure 3, NGC 4206’s NC has sufficient size and luminosity, even after modest age fading, to be a UCD progenitor. The galaxy threshing scenario has also been shown to be feasible by Côté et al. (2006) for dwarf elliptical nuclei, although De Propriis et al. (2005) suggests that dE,N are in general more compact than UCDs. One of the galaxy nuclei they study does have similar properties to the UCDs, as well as possessing spiral arms which indicate the galaxy may be an anemic spiral.

### 7.3. Connection to Black Holes

As residents of the same neighborhoods, it is natural to suspect that there may be some connection between nuclear clusters and supermassive black holes (SMBHs). The presence of SMBHs in the nuclei of >30 galaxies have been confirmed through dynamical measurements of their masses (reviewed by Ferrarese & Ford 2005). The masses of SMBHs are known to correlate with the mass and/or velocity dispersion of the bulge component (the  $M_\bullet - \sigma$  relation, Ferrarese & Merritt 2000; Gebhardt et al. 2000). Recent work on nuclear clusters in both spiral and elliptical galaxies have shown a remarkably similar trend (Rossa et al. 2006; Côté et al. 2006; Ferrarese et al. 2006; Wehner & Harris 2006). For a large sample of nucleated elliptical galaxies, Côté et al. (2006) have shown that the nucleus accounts for  $0.30 \pm 0.04\%$  of the total galaxy mass. This fraction is very similar to the fraction of galaxy mass found in the SMBHs (Ferrarese et al. 2006). For this

reason, Côté et al. (2006), Ferrarese et al. (2006) and Wehner & Harris (2006) suggest that nuclear clusters and SMBHs be thought of as a single-class of *Central Massive Objects*. They suggest a transition at  $\sim 10^7 M_\odot$  between nuclear clusters and SMBHs. However, the detection of numerous lower mass SMBHs at the centers of early and late-type dwarf galaxies (Barth et al. 2005; Greene et al. 2005), and the co-existence of nuclear star clusters and SMBHs in NGC 4395 (Filippenko & Ho 2003) and perhaps in NGC 4206 (§6), suggest that this transition may not be abrupt.

The formation of black holes in the centers of nuclear clusters may be related to the intermediate mass black holes (IMBHs) found in the centers of massive non-nuclear star clusters. A  $1.7 \times 10^4 M_\odot$  black hole has been reported by Gebhardt et al. (2005) in the globular cluster G1 in Andromeda (which is also a possible stripped nuclei), based on stellar dynamics. A  $10^2$ - $10^4 M_\odot$  black hole has also been identified in one of M82’s young massive clusters, based on X-ray observations (Patruno et al. 2006). These black holes are thought to form either by early merging of massive young stars within the cluster, or by dynamical interaction in the core of the clusters over long time periods (Miller & Colbert 2004, and references therein). If IMBH formation is common in dense massive clusters, then nuclear clusters should frequently host black holes as well. Subsequent mergers of many IMBHs could then form supermassive black holes (SMBHs) (Miller & Colbert 2004). As the mass of the SMBH increases, these mergers will likely destroy the nuclear clusters (see §5.2.2 of Côté et al. 2006), distributing their stars into the bulge.

## 8. SUMMARY

We have examined the nuclear regions of fourteen nearby galaxies using HST/ACS images in the F606W and F814W filters. We find nuclear cluster candidates within  $2''$  of the photocenter of nine of these galaxies. We have also obtained multi-band photometry and a spectrum of the NGC 4244 nuclear cluster, the nearest object in our sample. Analyzing these nuclear clusters, we find the following:

1. From the edge-on perspective, three of the nine cluster candidates (IC 5052, NGC 4206, NGC 4244) have morphologies suggesting they have both disk and spheroidal components. These components are very compact with scale lengths and half-light radii of 2-30 pc. Star clusters with multiple visible components have not previously been seen.
2. The three multi-component nuclear clusters have elongations oriented to within  $\sim 10^\circ$  of the major-axis of the galaxy.
3. The magnitudes and sizes of the clusters in our edge-on sample are very similar to those observed in other face-on, late-type galaxies (Böker et al. 2004) and dE galaxies (Côté et al. 2006).
4. The spheroids of the multi-component nuclear clusters are 0.3-0.6 magnitudes redder than the disks in F606W-F814W. This color difference implies the disks are populated with stars <1 Gyr in age.

5. Fitting single-stellar population models to the spectral and photometric data of the NGC 4244 nuclear cluster, we find it is best-fit by ages of  $\sim 70$  Myr or  $\sim 0.8$  Gyr. The implied total mass of the cluster for is  $\sim 3 \times 10^6 M_{\odot}$ .
6. A combination of two or more stellar populations significantly improves the fit to the NGC 4244 nuclear cluster spectral and photometric data. In the multi-age fits, the youngest ( $\lesssim 100$  Myr) stellar population matches the luminosity of the disk component, and appears to make up  $\lesssim 5\%$  of the total mass of the cluster. As much as  $\sim 10^7 M_{\odot}$  of old (10 Gyr) stars may also be present in the cluster. A constant star formation rate over the last 12 Gyr also provides a surprisingly good fit.
7. Using an HII region 19 pc from the center of the NGC 4244 NC, we measure the velocity offset of emission and absorption components in our spectrum to obtain a lower limit to the dynamical mass for the nuclear cluster of  $2.5_{-1.2}^{+1.7} \times 10^6 M_{\odot}$ .
8. Analysis of emission lines in the NGC 4206 nucleus suggest that it may host an AGN as well as a stellar

cluster.

These observational results strongly support an *in situ* formation model for nuclear star clusters. We suggest a specific model in which stars are formed episodically when gas accretes into a compact nuclear disk. After formation the stars gradually lose angular momentum and eventually end up in a spheroidal component. We show that a duty cycle for star formation of  $\sim 0.5$  Gyr is consistent with our and previous observations. The angular momentum must also be lost on this timescale, which we suggest may occur due to interactions of the nuclear cluster with the surrounding galaxy potential.

Acknowledgments: The authors would like to thank their anonymous referee, Carl-Jakob Walcher, Thomas Puzia, Tom Quinn, and Nate Bastian for their helpful comments on improving this manuscript. We also thank Leo Girardi for his help in interpreting models, Andrew West for his help with SDSS, Kevin Covey for fruitful discussions, and Roelof de Jong for his ongoing support. This work has been supported by HST-AR-10309, HST-GO-9765, the Sloan Foundation, and NSF grant CAREER AST 02-38683.

#### REFERENCES

- Agekian, T. A. 1958, *Soviet Astronomy*, 2, 22
- Barth, A. J., Greene, J. E., & Ho, L. C. 2005, *ApJ*, 619, L151
- Bastian, N., Saglia, R. P., Goudfrooij, P., Kissler-Patig, M., Maraston, C., Schweizer, F., & Zoccali, M. 2006, *A&A*, 448, 881
- Beasley, M. A., Strader, J., Brodie, J. P., Cenarro, A. J., & Geha, M. 2006, *AJ*, 131, 814
- Bedin, L. R., Piotto, G., Anderson, J., Cassisi, S., King, I. R., Momany, Y., & Carraro, G. 2004, *ApJ*, 605, L125
- Bekki, K., & Chiba, M. 2004, *A&A*, 417, 437
- Bekki, K., Couch, W. J., & Drinkwater, M. J. 2001, *ApJ*, 552, L105
- Bekki, K., Couch, W. J., & Shioya, Y. 2006, *ApJ*, 642, L133
- Binney, J., & Tremaine, S. 1987, *Galactic dynamics* (Princeton, NJ, Princeton University Press, 1987, 747 p.)
- Böker, T., Forster-Schreiber, N. M., & Genzel, R. 1997, *AJ*, 114, 1883
- Böker, T., Krabbe, A., & Storey, J. W. V. 1998, *ApJ*, 498, L115+
- Böker, T., Laine, S., van der Marel, R. P., Sarzi, M., Rix, H.-W., Ho, L. C., & Shields, J. C. 2002, *AJ*, 123, 1389
- Böker, T., Sarzi, M., McLaughlin, D. E., van der Marel, R. P., Rix, H.-W., Ho, L. C., & Shields, J. C. 2004, *AJ*, 127, 105
- Bottinelli, L., Gouguenheim, L., Paturel, G., & de Vaucouleurs, G. 1985, *A&AS*, 59, 43
- Bottinelli, L., Gouguenheim, L., & Teerikorpi, P. 1988, *A&A*, 196, 17
- Bruzual, G., & Charlot, S. 2003, *MNRAS*, 344, 1000
- Cardelli, J. A., Clayton, G. C., & Mathis, J. S. 1989, *ApJ*, 345, 245
- Carlson, M. N., & Holtzman, J. A. 2001, *PASP*, 113, 1522
- Carollo, C. M., Stiavelli, M., Seigar, M., de Zeeuw, P. T., & Dejonghe, H. 2002, *AJ*, 123, 159
- Chabrier, G. 2003, *PASP*, 115, 763
- Côté, P. et al. 2006, arXiv:astro-ph/0603252
- Davidge, T. J., & Courteau, S. 2002, *AJ*, 123, 1438
- Davies, J. I., & Phillipps, S. 1988, *MNRAS*, 233, 553
- Davies, R. et al. 2006, arXiv:astro-ph/0604125
- Davoust, E., & Prugniel, P. 1990, *A&A*, 230, 67
- de Grijs, R., Fritze-v. Alvensleben, U., Anders, P., Gallagher, J. S., Bastian, N., Taylor, V. A., & Windhorst, R. A. 2003, *MNRAS*, 342, 259
- De Propris, R., Phillipps, S., Drinkwater, M. J., Gregg, M. D., Jones, J. B., Evstigneeva, E., & Bekki, K. 2005, *ApJ*, 623, L105
- Drinkwater, M. J., Gregg, M. D., Hilker, M., Bekki, K., Couch, W. J., Ferguson, H. C., Jones, J. B., & Phillipps, S. 2003, *Nature*, 423, 519
- Fall, S. M., & Frenk, C. S. 1985, in *IAU Symp. 113: Dynamics of Star Clusters*, 285–296
- Ferrarese, L. 2002, *ApJ*, 578, 90
- Ferrarese, L. et al. 2006, arXiv:astro-ph/0603840
- Ferrarese, L., & Ford, H. 2005, *Space Science Reviews*, 116, 523
- Ferrarese, L., & Merritt, D. 2000, *ApJ*, 539, L9
- Filippenko, A. V., & Ho, L. C. 2003, *ApJ*, 588, L13
- Garnett, D. R. 2002, *ApJ*, 581, 1019
- Gavazzi, G., Boselli, A., Scodreggio, M., Pierini, D., & Belsole, E. 1999, *MNRAS*, 304, 595
- Gebhardt, K. et al. 2000, *ApJ*, 539, L13
- Gebhardt, K., Rich, R. M., & Ho, L. C. 2002, *ApJ*, 578, L41
- . 2005, *ApJ*, 634, 1093
- Girardi, L. 2006, <http://pleiadi.pd.astro.it>
- Girardi, L., Grebel, E. K., Odenkirchen, M., & Chiosi, C. 2004, *A&A*, 422, 205
- Gnedin, O. Y., Zhao, H., Pringle, J. E., Fall, S. M., Livio, M., & Meylan, G. 2002, *ApJ*, 568, L23
- Grant, N. I., Kuipers, J. A., & Phillipps, S. 2005, *MNRAS*, 363, 1019
- Greene, J. E., Barth, A. J., & Ho, L. C. 2005, arXiv:astro-ph/0511810
- Harris, W. E. 1996, *AJ*, 112, 1487
- Harris, W. E., Harris, G. L. H., Holland, S. T., & McLaughlin, D. E. 2002, *AJ*, 124, 1435
- Harris, W. E., Whitmore, B. C., Karakla, D., Okoń, W., Baum, W. A., Hanes, D. A., & Kavelaars, J. J. 2006, *ApJ*, 636, 90
- Ho, L. C., Filippenko, A. V., & Sargent, W. L. 1995, *ApJS*, 98, 477
- Huxor, A. P., Tanvir, N. R., Irwin, M. J., Ibata, R., Collett, J. L., Ferguson, A. M. N., Bridges, T., & Lewis, G. F. 2005, *MNRAS*, 360, 1007
- Jensen, J. B., Tonry, J. L., Barris, B. J., Thompson, R. I., Liu, M. C., Rieke, M. J., Ajhar, E. A., & Blakeslee, J. P. 2003, *ApJ*, 583, 712
- Jones, J. B. et al. 2006, *AJ*, 131, 312
- King, I. 1961, *AJ*, 66, 68
- Kroupa, P. 2001, *MNRAS*, 322, 231
- Larsen, S. S. 1999, *A&AS*, 139, 393
- Lauer, T. R., Faber, S. M., Ajhar, E. A., Grillmair, C. J., & Scowen, P. A. 1998, *AJ*, 116, 2263
- Layden, A. C., & Sarajedini, A. 2000, *AJ*, 119, 1760
- Long, K. S., Charles, P. A., & Dubus, G. 2002, *ApJ*, 569, 204
- Longaretti, P.-Y., & Lagoute, C. 1997, *A&A*, 319, 839
- Lotz, J. M., Miller, B. W., & Ferguson, H. C. 2004, *ApJ*, 613, 262
- Lotz, J. M., Telford, R., Ferguson, H. C., Miller, B. W., Stiavelli, M., & Mack, J. 2001, *ApJ*, 552, 572
- Mackey, A. D., & van den Bergh, S. 2005, *MNRAS*, 360, 631

- Maaz, D., Barth, A. J., Sternberg, A., Filippenko, A. V., Ho, L. C., Macchetto, F. D., Rix, H.-W., & Schneider, D. P. 1996, *AJ*, 111, 2248
- Marigo, P. 2001, *A&A*, 370, 194
- Martini, P., & Ho, L. C. 2004, *ApJ*, 610, 233
- Mastropietro, C., Moore, B., Mayer, L., Debattista, V. P., Piffaretti, R., & Stadel, J. 2005, *MNRAS*, 364, 607
- Matthews, L. D. et al. 1999, *AJ*, 118, 208
- Meylan, G., & Mayor, M. 1986, *A&A*, 166, 122
- Meylan, G., Sarajedini, A., Jablonka, P., Djorgovski, S. G., Bridges, T., & Rich, R. M. 2001, *AJ*, 122, 830
- Mieske, S., Hilker, M., & Infante, L. 2002, *A&A*, 383, 823
- Miller, M. C., & Colbert, E. J. M. 2004, *International Journal of Modern Physics D*, 13, 1
- Milosavljević, M. 2004, *ApJ*, 605, L13
- Moore, B., Katz, N., Lake, G., Dressler, A., & Oemler, A. 1996, *Nature*, 379, 613
- Obric, M. et al. 2006, *ArXiv Astrophysics e-prints*
- Olling, R. P. 1996, *AJ*, 112, 457
- Patruno, A., Zwart, S. F. P., Dewi, J., & Hopman, C. 2006, *astro-ph/0602230*
- Paturel, G., Theureau, G., Bottinelli, L., Gouguenheim, L., Coudreau-Durand, N., Hallet, N., & Petit, C. 2003, *A&A*, 412, 57
- Paturel, G. et al. 1995, *LEDA: The Lyon-Meudon Extragalactic Database (ASSL Vol. 203: Information On-Line Data in Astronomy)*, 115–126
- Phillipps, S., Drinkwater, M. J., Gregg, M. D., & Jones, J. B. 2001, *ApJ*, 560, 201
- Rossa, J., van der Marel, R. P., Boeker, T., Gerssen, J., Ho, L. C., Rix, H.-W., Shields, J. C., & Walcher, C.-J. 2006, *astro-ph/0604140*
- Saha, A., Claver, J., & Hoessel, J. G. 2002, *AJ*, 124, 839
- Sarzi, M., Rix, H.-W., Shields, J. C., Ho, L. C., Barth, A. J., Rudnick, G., Filippenko, A. V., & Sargent, W. L. W. 2005, *ApJ*, 628, 169
- Schinnerer, E., Böker, T., & Meier, D. S. 2003, *ApJ*, 591, L115
- Schlegel, D. J., Finkbeiner, D. P., & Davis, M. 1998, *ApJ*, 500, 525
- Seth, A. C., Dalcanton, J. J., & de Jong, R. S. 2005, *AJ*, 129, 1331
- Shapiro, S. L., & Marchant, A. B. 1976, *ApJ*, 210, 757
- Sirianni, M. et al. 2005, *PASP*, 117, 1049
- Smith, V. V. 2004, in *Origin and Evolution of the Elements*, ed. A. McWilliam & M. Rauch, 186–
- Thatte, N., Quirrenbach, A., Genzel, R., Maiolino, R., & Tecza, M. 1997, *ApJ*, 490, 238
- Tonry, J. L., Dressler, A., Blakeslee, J. P., Ajhar, E. A., Fletcher, A. B., Luppino, G. A., Metzger, M. R., & Moore, C. B. 2001, *ApJ*, 546, 681
- Trager, S. C., King, I. R., & Djorgovski, S. 1995, *AJ*, 109, 218
- Tremaine, S. D., Ostriker, J. P., & Spitzer, L. 1975, *ApJ*, 196, 407
- Tully, R. B., & Pierce, M. J. 2000, *ApJ*, 533, 744
- van der Kruit, P. C., & Searle, L. 1981, *A&A*, 95, 105
- Walcher, C.-J., Boeker, T., Charlot, S., Ho, L. C., Rix, H.-W., Rossa, J., Shields, J. C., & van der Marel, R. P. 2006, *astro-ph/0604138*
- Walcher, C. J. et al. 2005, *ApJ*, 618, 237
- Wehner, E., & Harris, W. 2006, *arXiv:astro-ph/0603801*